Molecular Phylogenetics and Evolution 120 (2018) 375–389

Contents lists available at ScienceDirect

Molecular Phylogenetics and Evolution

journal homepage: www.elsevier.com/locate/ympev

Molecular systematics and biogeography of lowland antpittas (Aves, Grallariidae): The role of vicariance and dispersal in the diversification of a widespread Neotropical lineage

Lincoln Carneiro[a,g,*], Gustavo A. Bravo[b,c,d], Natalia Aristizábal[b,c,e], Andrés M. Cuervo[b,c,f], Alexandre Aleixo[g]

[a] Curso de Pós-Graduação em Zoologia, Universidade Federal do Pará–Museu Paraense Emílio Goeldi, Belém, Pará, Brazil
[b] Museum of Natural Science, Louisiana State University, Baton Rouge, LA 70803, USA
[c] Department of Biological Sciences, Louisiana State University, Baton Rouge, LA 70803, USA
[d] Department of Organismic and Evolutionary Biology & Museum of Comparative Zoology, Harvard University, Cambridge, MA 02138, USA
[e] Departamento de Ecologia, Instituto de Biociências, Universidade de São Paulo, São Paulo, SP 05508-900, Brazil
[f] Instituto de Investigación de Recursos Biológicos Alexander von Humboldt, Villa de Leyva, Colombia
[g] Coordenação de Zoologia, Museu Paraense Emílio Goeldi, Caixa Postal 399, CEP 66040-170 Belém, Pará, Brazil

ARTICLE INFO

Keywords:
Amazonia
Ancestral range estimation
Dispersal
Diversification rates
Plio-Pleistocene
Phylogeny

ABSTRACT

We infer phylogenetic relationships, divergence times, and the diversification history of the avian Neotropical antpitta genera *Hylopezus* and *Myrmothera* (Grallariidae), based on sequence data (3,139 base pairs) from two mitochondrial (ND2 and ND3) and three nuclear nuclear introns (TGFB2, MUSK and FGB-I5) from 142 individuals of the 12 currently recognized species in *Hylopezus* and *Myrmothera* and 5 outgroup species. Phylogenetic analyses recovered 19 lineages clustered into two major clades, both distributed in Central and South America. *Hylopezus nattereri*, previously considered a subspecies of *H. ochroleucus*, was consistently recovered as the most divergent lineage within the *Grallaricula/Hylopezus/Myrmothera* clade. Ancestral range estimation suggested that modern lowland antpittas probably originated in the Amazonian Sedimentary basin during the middle Miocene, and that most lineages within the *Hylopezus/Myrmothera* clade appeared in the Plio-Pleistocene. However, the rate of diversification in the *Hylopezus/Myrmothera* clade appeared to have remained constant through time, with no major shifts over the 20 million years. Although the timing when most modern lineages of the *Hylopezus/Myrmothera* clade coincides with a period of intense landscape changes in the Neotropics (Plio-Pleistocene), the absence of any significant shifts in diversification rates over the last 20 million years challenges the view that there is a strict causal relationship between intensification of landscape changes and cladogenesis. The relative old age of the *Hylopezus/Myrmothera* clade coupled with an important role ascribed to dispersal for its diversification, favor an alternative scenario whereby long-term persistence and dispersal across an ever-changing landscape might explain constant rates of cladogenesis through time.

1. Introduction

In recent years, several features of land surface evolution have been invoked to explain Neotropical biogeographic patterns. For instance, changes in drainage and sedimentation patterns within large wetlands in western Amazonia during the Miocene (Figueiredo et al., 2009; Hoorn et al., 2013; Jaramillo et al., 2017; Wesselingh et al., 2002), and the Andean uplift unleashed climate changes across the continent (e.g., Insel et al., 2009) that ultimately affected current distributional patterns of a wide array of organisms (Antonelli and Sanmartín, 2011; Hoorn et al., 2013, 2010). Given this scenario, closely related taxa distributed across different Neotropical biomes offer good opportunities not only to infer their biogeographic history, but also to shed light on the processes underlying biological diversification of Neotropical biotas (Aleixo, 2004; D'Horta et al., 2012; Fernandes et al., 2014). Furthermore, the advent of event-based biogeography now allows the integration of all relevant processes (i.e. dispersal, extinction, vicariance, and founder-event speciation) through the use of explicit models (Matzke, 2014; Sanmartín et al., 2008). These event-based estimations specify both the ancestral distributions and associated causal events,

* Corresponding author at: Coordenação de Zoologia, Museu Paraense Emílio Goeldi, Caixa Postal 399, CEP 66040-170 Belém, Pará, Brazil.
E-mail addresses: lincoln_carneiro@yahoo.com.br (L. Carneiro), gustavo_bravo@fas.harvard.edu (G.A. Bravo), nati.aristizabal11@gmail.com (N. Aristizábal), amcuervo@gmail.com (A.M. Cuervo), aleixo@museu-goeldi.br (A. Aleixo).

https://doi.org/10.1016/j.ympev.2017.11.019
Received 3 July 2017; Received in revised form 16 October 2017; Accepted 28 November 2017
Available online 09 December 2017
1055-7903/

thus making it easier to compare alternative evolutionary/biogeographical scenarios (Matzke, 2014; Ronquist and Sanmartín, 2011; Sanmartín et al., 2008).

Passerine understorey birds with low dispersal propensity are good models for testing biogeographical hypotheses because they are particularly susceptible to be delimited by geographical barriers, such as rivers and mountains (Aleixo, 2004; Burney and Brumfield, 2009; Winger et al., 2015). The Grallariidae (*sensu* Moyle et al., 2009a; Rice, 2005), commonly known as antpittas, is a Neotropical family of suboscine passerines that comprises ~50 species restricted primarily to the understorey of forested habitats in tropical South and Central America. They are known for their secretive behavior and their tendency to have small distribution ranges that, in combination with their rotund body, long legs, and short wings and tail, suggest they are poor dispersers (Krabbe and Schulenberg, 2003). In fact, recent biogeographic analyses support the notion that current distribution ranges of Andean antpittas are consistent with the idea of vicariant speciation, rather than dispersal events across pre-existing barriers (Winger et al., 2015). Recent DNA-based phylogenies support the monophyly of the family (Moyle et al., 2009a; Ohlson et al., 2013; Rice, 2005), which is also partially supported by morphological characters (Ames, 1971; Galvão and Gonzaga, 2011; Lowery and O'Neil, 1969). Antpittas are currently organized into the genera *Grallaria*, *Grallaricula*, *Myrmothera*, and *Hylopezus* (Remsen et al., 2017), and molecular data suggest that *Hylopezus* and *Myrmothera* are sister taxa, that *Grallaricula* is their closest relative, and that this entire clade is sister to *Grallaria* (Moyle et al., 2009a; Ohlson et al., 2013; Rice, 2005).

In this study, we inferred phylogenetic relationships, divergence times, and the biogeographic history of the lowland genera *Hylopezus* and *Myrmothera* using mitochondrial and nuclear loci. We inferred biogeographic patterns and estimated a comprehensive time-calibrated phylogeny for these genera. We also estimated ancestral distributional ranges and tested for temporal shifts in diversification rates. Our main goal was to verify whether major late Miocene and Plio-pleistocene landscape changes in the Neotropics (e.g., uplift of the Andes and the consolidation of the modern Amazonian trans-continental drainage) were correlated with diversification in this widespread lineage, as inferred for other Neotropical taxa (Brumfield and Edwards, 2007; Lima et al., 2017; Ribas and Miyaki, 2007; Smith et al., 2014). A central prediction derived from the purported correlation between landscape change events and diversification is that cladogensis is expected to accelerate as a direct response to increased opportunities for vicariance following the appearance of novel barriers (Chaves et al., 2011; Moore and Donoghue, 2007; Weir and Price, 2011).

2. Material and methods

2.1. Taxon sampling and molecular phylogeny

To infer phylogenetic relationships within *Hylopezus* and *Myrmothera*, we sequenced a total of 142 vouchered individuals (76 *Hylopezus*, 61 *Myrmothera,* 2 *Grallaricula,* 3 *Grallaria*) from localities throughout their distributions (Figs. A1 and A2, Table A1). Our sampling spanned the geographical distributions of all 12 currently recognized species within *Hylopezus* (10) and *Myrmothera* (2) (Carneiro et al., 2012; Krabbe and Schulenberg, 2003; Remsen et al., 2017). We included as outgroups five samples from the two other genera currently recognized in the Grallariidae (Krabbe and Schulenberg, 2003; Rice, 2005): *Grallaricula* (*G. flavirostris* and *G. nana*) and *Grallaria* (*G. rufula*, *G. ruficapilla* and *G. guatimalensis*). The choice of *Grallaria* and *Grallaricula* taxa included in the analyses was guided by a complete and yet unpublished phylogeny of the Grallariidae family (Bravo et al. in prep).

Total genomic DNA was extracted using DNeasy tissue extraction kits (Qiagen, Valencia, CA, USA). For most samples, we sequenced the mitochondrial genes – NADH dehydrogenase subunit 2 (ND2: 1,041 base pairs, bp), and NADH dehydrogenase subunit 3 (ND3: 351 bp). We also sequenced three nuclear introns representing the main lineages inferred from our complete mtDNA data, as follows: transforming growth factor beta 2 intron 5 (TGFB2: 625 bp); the 3rd intron of the Z-linked muscle-specific kinase (MUSK: 582 bp); and a fragment of the beta-fibrinogen intron 5 (FGB-I5: 549 bp). We used standard methods described elsewhere (Brumfield et al., 2007; Brumfield and Edwards, 2007; Kimball et al., 2009) to amplify and obtain sequences for these five markers. For primer details see Table A2.

Electropherograms were inspected, assembled in contigs and edited in Geneious 9.1.2 (http://www.geneious.com, Kearse et al., 2012). Sequences were aligned with MAFFT v. 6 (Katoh et al., 2002) using the default parameters, and further inspected visually. Heterozygous sites were coded according to IUPAC when double peaks were present in both strands of the same individual's electropherograms. The softwares used in our phylogenetic inferences treat by default IUPAC codes of DNA base combinations as missing data (Potts et al., 2014). Simulations and empirical analysis suggest that this magnitude of missing data (< 0.5% in our case) does not affect phylogenetic estimates at the scale carried out herein (Wiens and Moen, 2008).

2.2. Phylogeny estimation

To identify geographical lineages to be used in subsequent analyses, we generated a concatenated multilocus phylogeny including all individuals sampled (n = 142 including outgroups) using Bayesian inference (BI) on MrBayes 3.2.1 (Ronquist et al., 2012). In this analysis only three species of the genus *Grallaria* were chosen to root the tree.

Lineages were defined as population clusters separated by pairwise genetic distances equal to or greater than that separating the sister species pair of lowland antpittas *H. whittakeri* and *H. paraensis*, which are also distinguished by conspicuous vocal differences (Carneiro et al., 2012). We accepted values of Bayesian posterior probability ≥0.95 as statistically well-supported nodes (Bryson et al., 2014; Huelsenbeck and Rannala, 2004).

Models of molecular evolution and best-fit partitioning schemes were selected using the Bayesian Information Criterion (BIC) (Minin et al., 2003) as implemented in PartitionFinder V1.1.1 (Lanfear et al., 2012). We defined separate data blocks for the three codon positions of the protein-coding genes (ND2, ND3) and a single data block for each intron (TGFB2, MUSK, FGB-I5). The optimal partition scheme and the best-fit models used on the BI are described in details in the Appendix (Table A3). Two independent runs were conducted, each with three heated and one cold Markov chain sampling every 1000 generations for 20 million generations. Output parameters were visualized using Tracer 1.6 (Rambaut et al., 2014) to evaluate stationarity and convergence (Effective Sample Size – ESS values > 200). We further assessed convergence between runs using the 'RWTY' package, which implements functions of the AWTY in the R environment (https://github.com/danlwarren/RWTY; Nylander et al., 2008). The first 25% of generations were discarded as burn-in. MrBayes analyses were carried out in the CIPRES Science Gateway (Miller et al., 2010).

2.3. Species trees and divergence time estimate

We used ∗BEAST (Heled and Drummond, 2010), part of the BEAST 1.7.4 package (Drummond et al., 2012), to generate a time-calibrated species tree and a mtDNA chronogram, using all individuals from each currently recognized species or geographical lineages recovered by our MrBayes analysis. Following recommendations contained in the BEAST manual (Drummond et al., 2012), we did not root the tree in any specific outgroup. We considered the same partitions and models estimated in our PartitionFinder analysis.

We used a Yule speciation prior and a relaxed uncorrelated log-normal clock for each gene tree (Drummond et al., 2006). We applied two different calibration strategies to obtain absolute divergence times. First, we constrained the ages of relevant nodes based on normally

distributed priors of dates estimated by Ohlson et al., (2013) for the New World suboscines: (1) crown age of the Grallariidae set to 26.2 Ma (95% confidence interval: 24.56–27.84); (2) crown age of the genus *Grallaria* set to 20.4 Ma (95% confidence interval: 18.76–22.04); and (3) crown age of the clade comprising *Grallaricula*, *Myrmothera* and *Hylopezus* set to 17.1 Ma (95% confidence interval: 15.46–18.74). Second, we used the ND2 mutation rate of 1.25×10^2 substitutions/site/Myr (2.5% divergence between lineages per Myr) from Smith and Klicka (2010), for mitochondrial dataset (ND2, ND3), and of 1.35 x 10^3 substitutions/site/Myr for autosomal markers (MUSK, TGFB2, FGB-I5) from Ellegren (2007). We specified a lognormal distribution and a relatively wide logarithmic standard deviation of 0.2 for each gene, thus encompassing alternative substitution rates (e.g. Lerner et al., 2011). We performed two independent runs with 1.2×10^9 generations each, with parameters sampled every 10,000 generations and a burn-in of 10%.

We generated a second species tree using only the full mtDNA dataset to estimate divergences based on all 142 specimens of lowland antpittas sampled and the five outgroups. Although mtDNA provides only a single-gene estimate of a species tree, ∗BEAST can estimate divergence times from mtDNA data that account for gene divergences that may pre-date species divergences (Bryson et al., 2014; Heled and Drummond, 2010). Because we could not amplify all nuclear markers for all taxa (i.e., only mtDNA sequences were obtained for *H. perspicillatus* and *H. dilutus*), this approach allowed us to estimate a phylogeny and a chronogram from a taxonomically more complete dataset. Following the same approach as outlined above, we used the same calibration strategy for the mtDNA markers and each specimen was assigned to a currently recognized species or geographical lineage inferred from our concatenated tree. Two independent runs with 1.5×10^8 generations each, with parameters sampled every 10,000 generations and a burn-in of 10% were performed.

For both multilocus and mtDNA species trees, we checked for convergence between runs and analyses performance using Tracer 1.6, and accepted the results if ESSs values were > 200. The parameter values of the samples from the posterior distribution were summarized on a maximum clade credibility tree using TreeAnnotator 1.7.4 (Drummond and Rambaut, 2007).

2.4. Ancestral range estimation

To estimate the biogeographic history of distributional ranges of lowland antpittas across the Neotropics, we used 'BioGeoBEARS (Biogeography with Bayesian (and likelihood) Evolutionary Analysis' in R Scripts; Matzke, 2013; http://cran.r-project.org/web/packages/BioGeoBEARS/index.html). This package uses a maximum likelihood method similar to that implemented in the software LAGRANGE (Ree and Smith, 2008). In this inference, ancestral ranges are optimized onto internal nodes.

BioGeoBEARS implements many models in a common likelihood framework, so that standard statistical model selection procedures can be applied to let the data choose the best model (Matzke, 2013). We performed a total of six different analyses including the Dispersal-Extinction Cladogenesis Model (DEC), a likelihood version of the Dispersal-Vicariance Analysis ("DIVALIKE"), and a version of the Bayesian inference of historical biogeography for discrete areas (BAYAREALIKE), as well as "+J" versions of these three models, which include founder event speciation, an important process left out of most inference methods (Matzke, 2013). DEC, DIVALIKE, and BAYAREA each have two free parameters (*d* and *e*) specifying the rate of "dispersal" (range expansion) and "extinction" (range contraction) along phylogeny branches. For additional implementation details see Matzke (2013).

We defined nine biogeographical areas based on evidence available for historical relationships between relevant geographic areas in the Neotropics (Hoorn et al., 2010; Morrone, 2014), and on the current distribution of antpitta lineages. These biogeographic regions were adapted from Morrone (2014) as follows: Andes, Chocó, Central America, Tepuis, Guiana Shield, Amazon Sedimentary Basin, Brazilian Shield, South of Atlantic Forest, and Caatinga. The maximum possible number of ancestral states that could be assigned to each node was set to nine, so that each taxon or node could occur simultaneously in all pre-defined areas (Table A4). Our multilocus species tree was used to infer the ancestral range probabilities, which were computed for each node and subsequently plotted on the majority-rule chronogram. For the node pie charts of biogeographic ancestral ranges, we accepted probability values in which the most likely area was at least twice that of the second most likely area. The genus *Grallaria* was excluded from this analysis due to insufficient representation of their diversity in our sampling, which could mislead biogeographic estimates. Finally, we compared the six different models for statistical fit via comparison of Log-Likelihood (ln *L*), Akaike Information Criterion (AIC), ΔAIC, and Akaike weight (ω*i*) values.

Dispersal (d), Extinction (e), Founder (J), Log-Likelihood (ln *L*) and Akaike Information Criterion (AIC) values were directly obtained from BioGeoBEARS, whereas Akaike weight (ω*i*) and ΔAIC values were subsequently calculated from (AIC) values (Wagenmakers and Farrell, 2004).

2.5. Lineage diversification analyses

We used the 'APE', 'GEIGER' and the 'LASER' packages (Harmon et al., 2008; Paradis et al., 2004; Rabosky, 2006) in R (R Core Team, 2016) to describe lineage diversification within the clade comprising *Grallaricula*, *Hylopezus* and *Myrmothera*. We fitted a total of eight diversification models implementing two constant rates (pure birth and birth–death) and three variable rates (exponential and logistic density-dependent and two-rate pure birth) using 'LASER' 2.4 (Rabosky, 2006). The SPVAR, EXVAR and BOTHVAR models that allow differential extinction and speciation rates were measured following (Rabosky and Lovette, 2008). The models fit were ranked by comparison of values of Log-Likelihood (ln *L*), Akaike Information Criterion (AIC), ΔAIC, and Akaike weight (ω*i*). We generated lineage-through-time (LTT) plots to visualize the tempo of diversification within the *Hylopezus/Myrmothera* clade inferred from our multilocus species tree. These approaches were implemented to identify points in phylogeny that display significant shifts in diversification rates.

3. Results

3.1. Phylogeny

The genus *Hylopezus*, as currently defined, is polyphyletic (Fig. 1). Our results show that the genera *Hylopezus* and *Myrmothera* belong in three distinctive clades, which from now on will be referred to respectively as *Hylopezus nattereri*, the "core *Hylopezus* clade" (Fig. A1) and the "extended *Myrmothera* clade" (Fig. A2). The 'core *Hylopezus*' clade was found to contain seven lineages from eight currently recognized *Hylopezus* species, whereas the 'extended *Myrmothera*' clade comprises eight lineages from five species, including three taxa currently allocated in *Hylopezus* (Fig. 1; Krabbe and Schulenberg, 2003).

BI and the multilocus ST recovered the 'core *Hylopezus*' clade as sister to the 'extended *Myrmothera*' clade (PP = 1). Furthermore, *Hylopezus nattereri* was recovered with high support (PP = 1) as a distinct lineage within the *Hylopezus/Myrmothera* + *Grallaricula* clade, but its placement is uncertain, as demonstrated by the low posterior probability associated with the node at the base of *Grallaricula* and the *Hylopezus/Myrmothera* clades (Fig. 1).

Our reconstructions revealed all species currently recognized in the *Hylopezus/Myrmothera* clade as monophyletic, except for the paraphyly found within the genus *Myrmothera*. The widespread lowland Amazonian endemic *Myrmothera campanisona* was recovered as paraphyletic with respect to *M. simplex* and includes three distinct lineages

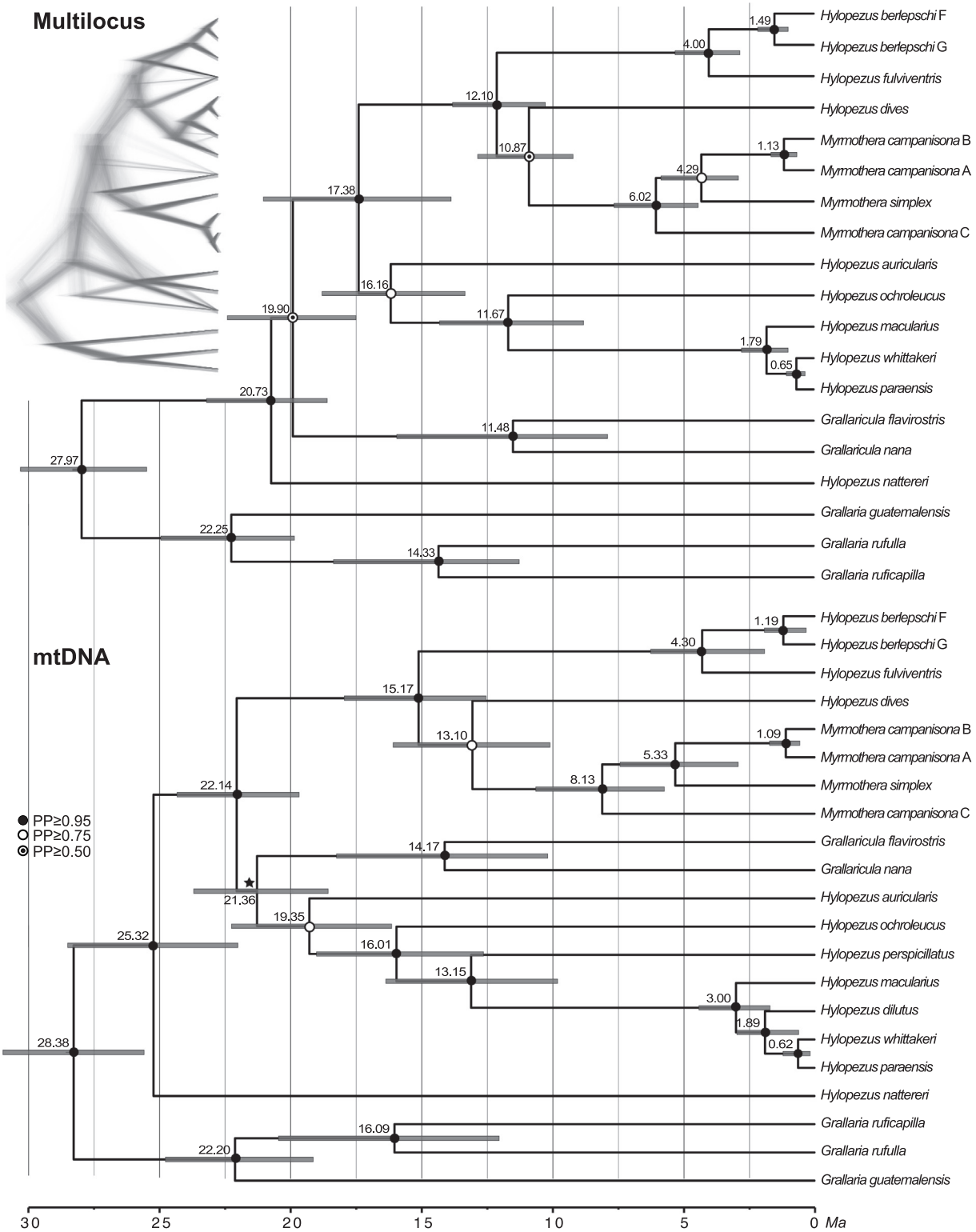

Fig. 1. Phylogenetic hypotheses estimated for antpittas from multilocus (species tree) and mtDNA (chronogram) datasets using *BEAST. Bars indicate 95% highest posterior densities of divergence dates. The mean estimated dates are shown above nodes and the scale bar is in millions of years ago (Ma). Bayesian posterior probability (PP) support for nodes are indicated by coded circles according to the figure legend, with nodes receiving less than 0.50 support marked with an asterisk. The inset (upper left) figure is the result of the superposition of all gene trees and has the same topology of the multilocus tree (generated by DensiTree 2.0.1).

subdivided into two groups: one comprising Guianan Shield and western Amazonian populations (lineage C), and another one (lineages A and B) comprising eastern Amazonian populations found east of the Madeira River. The latter was recovered as sister of the only other species in the genus, the highland Tepui endemic *M. simplex* (Fig. 1).

3.2. Species trees and divergence time estimation

Complete genetic data could not be obtained for some specimens used in our multilocus species tree analyses. In particular, we could not obtain FGB-I5 sequences from *H. dilutus* and any MUSK sequence from

H. perspicillatus (Fig. 1), thus, these taxa were only included in the mtDNA species tree analysis. Our multilocus species tree produced a time-calibrated phylogenetic tree with overall high resolution (Fig. 1). However, our multilocus and mtDNA chronogram topologies were quite different, particularly on the relationships between *Grallaricula* and members of the *Hylopezus/Myrmothera* clades (Fig. 1). The multilocus species tree also yielded high support for a relationship that was poorly supported in the mtDNA reconstruction: 'core *Hylopezus*' and 'extended *Myrmothera*' clades were recovered as sister groups.

Estimates of time divergences differed between the mtDNA and the multilocus species tree (Fig. 1). Mean estimated divergence dates in the mtDNA chronogram were younger; this was expected because mtDNA tends to coalesce faster than nuclear genes (Edwards and Beerli, 2000); however, the confidence intervals of time estimation on the mtDNA and the multilocus dataset overlap (Fig. 1). Based on the assumption that multilocus estimations of species trees are more robust, reliable, and more faithful to the history of lineages, and that they bring maternal and paternal information across independent loci, we decided to frame our estimations of divergence times and biogeographic estimates within the species tree produced by the multilocus dataset.

The multilocus species tree suggested an Oligocene divergence of the genus *Grallaria* from the remaining lineages in the family (mean estimated date 27.9 Ma, 95% HPD: 30.3–25.4 Ma), which diversified subsequently throughout the Early Miocene, as follows: (i) *H. nattereri* split at *c*. 20.7 Ma (95% HPD: 23.1–18.5 Ma); (ii) *Grallaricula* originated at *c*. 11.4 Ma (95% HPD: 15.9–7.8 Ma); and (iii) the *Hylopezus/Myrmothera* clade appeared at *c*. 17.3 Ma (95% HPD: 21.0–13.8 Ma). Diversification within the 'core *Hylopezus*' clade began with the early split of *H. auricularis* at *c*. 16.1 Ma (95% HPD: 18.7–13.3 Ma), and continued on through the late Miocene with the *H. ochroleucus* divergence at *c*. 11.6 Ma (95% HPD: 14.2–8.7 Ma). The estimates for divergence within the 'core *Hylopezus*' during the Pleistocene onwards differed between mtDNA and the multilocus analyses due to differences between the number of lineages sampled in each analysis (Fig. 1). Within the 'extended *Myrmothera*' clade divergence began during the late Miocene at *c*. 12.1 Ma (95% HPD: 13.7–10.2 Ma), and continued on throughout the Pliocene and into the Pleistocene (Fig. 1).

3.3. Diversification rates

Birth–death likelihood analyses of lineage diversification rates failed to reject the null hypothesis of rate constancy for multilocus species tree. We obtained pure birth as the best-fit model (Table 1). The lineage diversification rate in lowland antpittas remained constant through time, with diversification rates estimated at 0.091 divergence events per lineage per million years. The lineage-through-time plot also suggest a near constant diversification rate without significant shifts during most of the 20 million years history of the group (Fig. A3).

Table 1
Maximum likelihood analysis of diversification rates in the multilocus species tree for the *Grallaricula*, *Hylopezus* and *Myrmothera* clade (*Grallaria* genus excluded). Rate-constant and rate-variable models of diversification fit to the ultrametric phylogeny. Log-Likelihood (ln *L*), Akaike Information Criterion (AIC), ΔAIC, and Akaike weight (*ωi*) scores for each model are provided for each of the empirical LTTs. Rate-constant and rate-variable models providing the best fit are noted with bold.

Rank	Model	Parameters	ln *L*	AIC	ΔAIC	*ωi*
1	Pure-birth	1	−19.57	41.15	0	0.25
2	Diversity-dependent, exponential	2	−18.74	41.49	0.34	0.21
3	Yule-2-rate	3	−17.86	41.72	0.57	0.18
4	Diversity-dependent, linear	2	−19.11	42.22	1.07	0.14
5	Birth-death	2	−19.57	43.15	2	0.09
6	Speciation exponential decline	3	−19.18	44.37	3.22	0.05
7	Extinction exponential increase	3	−19.58	45.16	4.01	0.03
8	Variable speciation and extinction	4	−19.15	46.30	5.15	0.01

3.4. Ancestral range estimation

Of the six biogeographic models evaluated, the best fit to our dataset of lowland antpittas was DEC + J (ln $L = -51.26$). The node pie charts likelihoods of ancestral states, and the parameters and scores from each model implemented are given below (Fig. 2; Table 2). The recovered model (DEC) reflects a biogeographical framework in which daughter lineages inherit the ancestral ranges of the ancestors, allowing subset speciation, however without evidence of vicariance events. The founder-event (+J) is related to the colonization of new areas located beyond the limits of the most-probable ancestral distribution, like verified, for instance, in *H. ochroleucus* and *H. macularius* (Figs. 2 and 3).

The most-probable biogeographic estimation of ancestral ranges indicated that the common ancestor of lowland antpittas, *Grallaricula* and *H. nattereri*, occupied a considerable portion of the Neotropics, including four of the nine coded areas (Fig. 2). Our analysis suggested a subset speciation event during the early Miocene, which separated the Atlantic forest endemic *H. nattereri* from the remaining lineages. Still during the early Miocene, the diversification of the lineage that originated the genus *Grallaricula* took place. The most likely area of origin for the *Hylopezus/Myrmothera* clade (lowland antpittas) was the sedimentary basin in western Amazonia (Fig. 2). From this area, members of the *Hylopezus/Myrmothera* clade appeared to have colonized the remaining sectors of Amazonia and the Tepuis, as well as Trans-Andean South America, Central America and the northeastern Brazilian *Caatinga* biome (Figs. 2 and 3). However, as some nodes were statistically not well-supported in our phylogenetic hypotheses (such as those involving *H. dives* and *H. auricularis*) and some lineages were not included in the species tree (*H. dilutus* and *H. perspicillatus*), our estimation of ancestral ranges should be interpreted with caution.

4. Discussion

Our results contrast strongly with the current taxonomic status of the genera *Hylopezus* and *Myrmothera*, and suggest that *H. nattereri* should be treated as a highly divergent and independent lineage within Grallariidae, probably in a separate genus.

Although the timing when most modern lineages of the *Hylopezus/Myrmothera* clade appeared coincided with a period of intense landscape changes in the Neotropics (Plio-Pleistocene; Fig. 2), the absence of any significant shifts in diversification rates over the last 20 million years challenges the view that there is a strict causal relationship between intensification of landscape changes and cladogenesis (Table 1; Fig. A3). This finding is at odds with previous studies which coupled elevated rates of speciation with particular palaeogeographical or palaeoclimatic events (Chaves et al., 2011; Rull, 2008; Weir, 2006; Weir and Schluter, 2004) but agrees with others which have also documented steady rates of lineage accumulation up to the present (Bryson et al., 2014; Castroviejo-Fisher et al., 2014; D'Horta et al., 2012; Patel et al., 2011; Schweizer et al., 2014; Smith et al., 2014). However as previously pointed out by Tobias et al. (2008), such rate constancy patterns might be compromised by undetected cryptic lineages, which seems unlikely here considering the dense population level sampling employed, as well as the relatively recent divergences between lineages at the tips of branches in the multilocus phylogeny used in the analysis.

Given our data, and assuming the monophyly of the Grallariidae as supported by several studies (Galvão and Gonzaga, 2011; Moyle et al., 2009a; Ohlson et al., 2013; Rice, 2005), our ancestral range estimations suggest that the lowland antpitta clade originated in the western Amazonian sedimentary basin, which coincides with the group's modern stronghold, whereby most species are distributed in this area (Fig. 2).

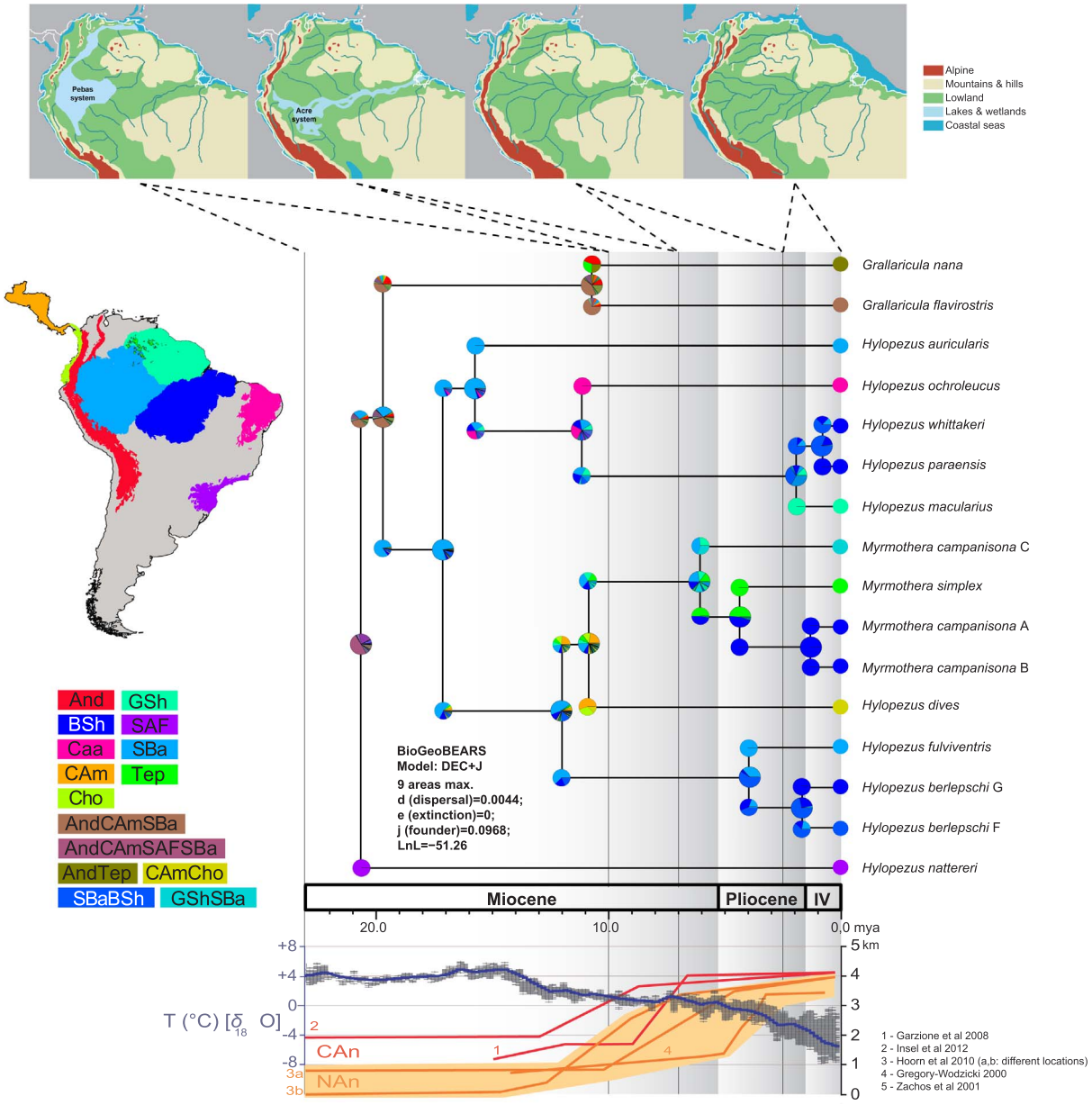

Fig. 2. Time-calibrated species trees generated by BEAST and ancestral range estimates provided by BioGeoBEARS, both derived from the multilocus dataset. The best-fit model for our ancestral range estimation was DEC + J (lnL = −51.26, AIC = 108.5). Node pie charts represent the likelihoods of ancestral states; the color-coded circles at the tips represent the current areas occupied by each lineage. IV = Quaternary. Lower panel (figure adpted from (Teixeira et al., 2016)): temperature changes (adapted from (Zachos et al., 2001) and Andean uplift (adapted from (Garzione et al., 2008; Gregory-Wodzicki, 2000; Hoorn et al., 2010; Insel et al., 2012). For additional details see Table A4).

Table 2
Models, parameters and scores from each of the analyses in BioGeoBEARS. Dispersal (d), Extinction (e), Founder (J), values of Log-Likelihood (ln *L*), Akaike Information Criterion (AIC), ΔAIC value, and Akaike weight (ω*i*).

Rank	Model	Parameters	d	e	j	ln *L*	AIC	ΔAIC	ω*i*
1	DEC + J	3	0.0044	1.00e−12	0.096	−51.26	108.5	0	0.91
2	DIVALIKE + J	3	0.0056	1.00e−12	0.090	−53.87	113.7	5.2	0.06
3	DEC	2	0.0079	1.63e−02	0	−56.71	117.4	8.9	0.01
4	DIVALIKE	2	0.0099	9.69e−03	0	−58.03	120.1	11.6	0
5	BAYAREALIKE + J	3	0.0051	8.12e−02	0.029	−57.68	121.4	12.9	0
6	BAYAREALIKE	2	0.0102	1.25e−01	0	−60.22	124.4	15.9	0

4.1. Origin and diversification of the Hylopezus/Myrmothera clade in the Neotropics

During the Early Miocene (*c.* 20 Ma), *H. nattereri* diverged from the remaining *Hylopezus* and *Myrmothera* lineages (Fig. 1). The divergence of the 'core *Hylopezus* clade' (which includes *H. auricularis, H. ochroleucus*, *H. perspicillatus*, *H. macularius*, *H. dilutus*, *H. whittakeri*, and *H. paraensis*; see Fig. 1) started during the Middle Miocene (*c.* 16 Ma) in the Sedimentary Basin of Western Amazonia and proceeded thereof to other parts of South America, eventually reaching Central America with

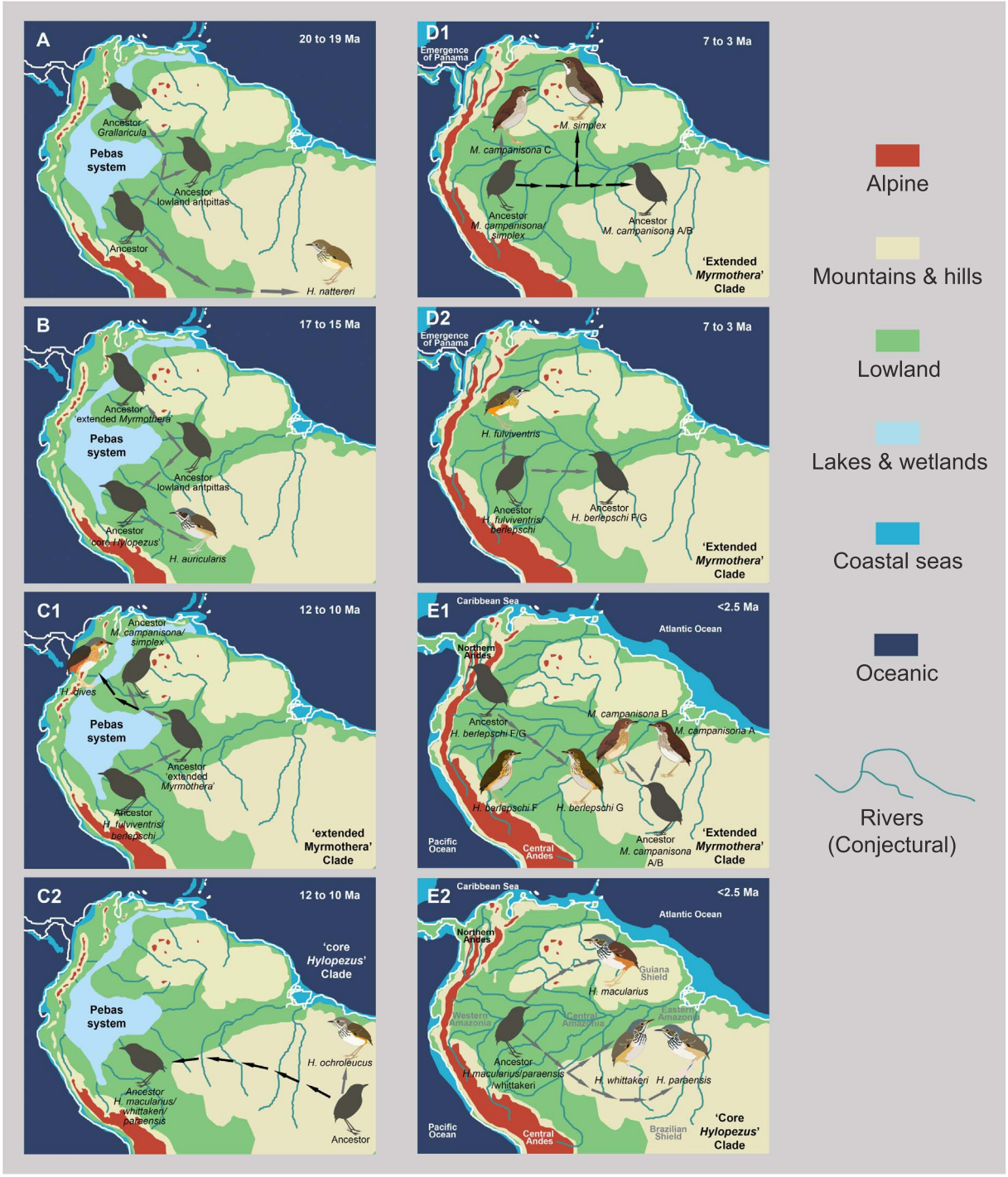

Fig. 3. Hypothesized palaeoscenarios for the evolution of the *Hylopezus/Myrmothera* clade. Palaegeographic maps follow Hoorn et al. (2010). (A; B; C1; C2) Miocene: Mountain building in the Central and Northern Andes (~12 Ma) and wetland propagation into Western Amazonia (Pebas system). (D1; D2) Late Miocene to Pliocene: the megawetland disappeared and upland *terra firme* rain forests expanded into western Amazonia; closure of Panama Isthmus, establishment of modern drainage of the Amazon river (Late Pliocene to Pleistocene; Campbell et al., 2006; Latrubesse et al., 2010) and final phase of Andean uplift. (E1; E2) Quaternary: the modern Amazon River is established and the Andean cordillera is uplifted. All currently extant *Hylopezus* and *Myrmothera* species diversified. The ancestors and the respective node codes follow Fig. 2. Arrows represent divergences in lineages, with gray and black arrows indicating divergences within and between distinct biogeographic areas, respectively. Images of antpittas species are adapted from Krabbe and Schulenberg (2003) and the Handbook of Birds of the World Alive.

H. perspicillatus. Independently, also during the middle Miocene (*c.* 12 Ma), the 'extended *Myrmothera* clade' (comprising *M. campanisona*, *M. simplex*, *H. dives*, *H. berlepschi*, and *H. fulviventris*; see Fig. 1) also began to diversify first in western Amazonia, reaching later trans-Andean South America and Central America (Figs. 2 and 3).

Despite the relatively high number of taxa in Grallariidae (51 species), a comparatively small number of species, essentially restricted to *Hylopezus*, *Myrmothera*, and *Grallaria* (*G. varia*, *G. eludens*, *G. dignissima*) occur in the lowlands (Krabbe and Schulenberg, 2003). To some other species-rich vertebrate groups, the Amazon basin has been postulated to act more like a sink than as primary source of diversity (Castroviejo-Fisher et al., 2014; Roy et al., 1997; Sedano and Burns, 2010). This imbalance in diversity between some Neotropical highland and lowland lineages can be related to the extinction of deep branches in

Grallariidae, as has also been inferred for other Suboscines lineages (Batalha-Filho et al., 2014; Ohlson et al., 2013). If more recent speciation events are clustered in the tectonically active highlands, geologically more stable lowland areas tend to accumulate older species (Roy, 1997), where extinction rates may not necessarily be higher. Even though comparing rates of cladogenesis between highland and lowland Grallariidae lineages is beyond the scope of this paper, our timing estimates for the origin of the *Hylopezus/Myrmothera* clade support a fairly ancient (Early Miocene) period for the onset of the diversification leading to the modern lowland antpittas.

On the other hand, niche conservatism can restrict lineage distribution and diversification to narrow geographic areas and environmental conditions (Giehl and Jarenkow, 2012). Thus, niche conservatism coupled with an overall low dispersal ability reported for some Grallariidae species (Stratford and Stouffer, 2015) could explain the relatively fewer number of extant lowland taxa in this family, when compared to some other widespread Neotropical lineages of similar ages, without necessarily resorting to events of extinction (Derryberry et al., 2011; Ohlson et al., 2013). However, it is crucial to distinguish the dispersal ability, associated with ecomorphological traits, from dispersal at large (i.e., evolutionary) time scales. Even species with strict ecological requirements and limited dispersion abilities may successfully colonize new areas over large time scales, as demonstrated for other continental and insular radiations (Clegg and Phillimore, 2010; Derryberry et al., 2011; Moyle et al., 2009b).

The diversification analysis indicated a best topological-fit to a pure birth model; even though two variable rates models (Diversity-dependent, exponential and Yule-2-rate) reached similar score values, our results suggest that neither declining speciation under low extinction nor increasing extinction under constant speciation can explain the pattern of lowland antpittas diversification (Table 1). This result is supported by model fitting in that neither the SPVAR nor the EXVAR (variable speciation or extinction through time) models received strong support. However, a more complex model of varying and irregular speciation and extinction rates could potentially generate a pattern nearly indistinguishable from a constant rate model (Derryberry et al., 2011; Rabosky and Lovette, 2008). The lowland antpittas diversification pattern mirrors that documented for at least another Neotropical avian continental radiation, which exhibited a similar pattern of nearly constant diversification throughout the Neogene and Quaternary (Derryberry et al., 2011). Together, these studies support that in at least two continental wide Neotropical radiations (Furnariidae and lowland Grallariidae), the dramatic changes in landscape that took place in the Miocene and early Pliocene (e.g., speed up at the rate of the Andean uplift and consolidation of the modern trans-continental Amazonian drainage) did not cause an acceleration in cladogenesis, implying that additional mechanisms other than barrier formation account for diversification in these groups. These findings are in agreement with interpretations of recent phylogeographic studies, which suggested that additional historical and natural history variables, such as age and dispersal capacity of a given lineage, are also keystone to explain the current megadiversity of Neotropical rainforests (Castroviejo-Fisher et al., 2014; Smith et al., 2014).

4.2. Diversification in the Amazon basin

Expansion from montane and higher latitude areas into the Amazon basin during the Early Miocene (Figs. 1–3) provided new opportunities for diversification within the Grallariidae. Despite reaching the Amazon basin around 19–20 Ma, most of the modern diversification within the *Hylopezus/Myrmothera* clade occurred more recently and simultaneously in both the 'core *Hylopezus* clade' and the 'extended *Myrmothera* clade' during two time frames. One oldest, between 10 and 17 Ma, within which these two major clades began to split. These older cladogenetic events may be related to more drastic changes in the Amazonian landscape, as the disappearance of the Pebas system and the consequent availability of habitats that followed (Hoorn et al., 2010). The second major episode of diversification seems to have begun at about 6 Ma, lasting until the Quaternary, and was probably more associated with the consolidation of the modern Amazonian drainage and climatic fluctuations of the Quaternary (Baker and Fritz, 2015; Hoorn et al., 2010). Posterior credibility intervals for 6 of the 12 divergences in our multilocus species tree encompass Pliocene and Quaternary dates. Our estimates of ancestral ranges of diversification for the *Hylopezus/Myrmothera* clade, point western Amazonia as the source of colonization events to other parts of the basin and neighboring areas, starting in the Middle Miocene (e.g., *H. ochroleucus* to Caatinga and *H. dives* to Central America; Figs. 1–3). Remarkable changes in the Amazonian landscape and the consolidation of its modern drainage (Hoorn et al., 2010) allowed the group to colonize (via dispersal) and diversify throughout the Amazon Basin (Figs. 2 and 3).

4.3. Diversification of the Atlantic Forest lineage

One of the early-diverging lineages in the *Hylopezus/Myrmothera* clade consists of the lone "*Hylopezus*" endemic taxon to the Atlantic Forest of southeastern South America: *H. nattereri* (Fig. 1). The origin of this lineage predates that of the *Hylopezus/Myrmothera* clade and was estimated as dating back to the Early Miocene (Figs. 1 and 3). Recent studies showed that the Atlantic Forest holds ancient lineages that date to the mid-Tertiary, as verified for birds (Derryberry et al., 2011), mammals (Fabre et al., 2013; Galewski et al., 2005), and frogs (Fouquet et al., 2012). This endemic Atlantic Forest lineage has an Andean component, and probably reached southeastern South America through the southern Andes, as it is restricted to humid subtropical and montane forests (Krabbe and Schulenberg, 2003).

4.4. Diversification of the Trans-Andean lineages

Our estimation of ancestral ranges suggests that *H. dives* originated from a western Amazonian ancestor that diversified in Trans-Andean South America/Central America after having dispersed across the Andes before its major uplift (mean estimated date 10.8 Ma, 95% HPD: 9.1–12.8 Ma; Fig. 1). However, it is important to note the poor support recovered for the *H. dives* node in both chronograms, and the topology differences between mtDNA and multilocus trees (Fig. 1). The dispersal across the Andes inferred for the ancestor of *H. dives* is consistent with the mountain building pattern, whereby orogeny followed a south to north direction (Hoorn et al., 2010), allowing a last burst of dispersal across the northern Andes (De-silva et al., 2016; Haffer, 1974; Scotti-saintagne et al., 2013). Although *H. perspicillatus* was not included in our ancestral range analysis, based on its modern distribution and phylogenetic position derived from mtDNA as a lineage closely related to an Amazonian endemic clade (Fig. 1), it seems plausible to assume that it split after a dispersal scenario similar to that postulated for *H. dives*. This pattern has also been invoked to explain the diversification of other avian groups across and along the Andes (Chaves et al., 2011; Ribas and Miyaki, 2007; Weir and Price, 2011).

4.5. Systematic implications

Results from our dense range-wide and taxonomic sampling molecular dataset shed new light into the systematics of antpittas. The 11 species of lowland antpittas currently recognized can be further divided into 3 additional geographically and genetically structured evolutionary units (Fig. 1).

At a broader level, our multilocus species tree strongly suggests that *Myrmothera* forms a monophyletic group that includes three species currently placed in the genus *Hylopezus* (*H. dives*, *H. fulviventris*, and *H. berlepschi*; Fig. 1). The clade formed by *H. auricularis*, *H. ochroleucus*, *H. whittakeri*, *H. paraensis*, and *H. macularius*, recovered by the multilocus species tree, probably also comprises *Hylopezus*' type species: *H.*

perspicillatus (Ridgway, 1909). Even though we had no success with the amplification of all nuclear markers for this taxon, it was recovered with high support within this clade according to both the concatenated Bayesian tree and the mtDNA chronogram (Fig. 1 and Fig. A1). Therefore, the following species must remain in *Hylopezus*: *H. auricularis*, *H. ochroleucus*, *H. perspicillatus, H. macularius, H. dilutus, H. whittakeri*, and *H. paraensis*.

The Atlantic forest endemic *H. nattereri* was recovered as an old and isolated lineage, not closely related to other species in *Hylopezus* and *Myrmothera* (Fig. 1). Nevertheless, *H. nattereri* was regarded until recently as a subspecies of *H. ochroleucus* based on plumage characters, being split later based on voice (Krabbe and Schulenberg, 2003; Whitney et al., 1995). Our phylogenetic estimates support the notion that plumage similarities between *H. nattereri* and *H. ochroleucus* could be result of convergence or simply retention of ancestral characters. We recommend the recognition of *H. nattereri* as a separate (monotypic) genus to be named elsewhere, given its large phylogenetic distance from the remaining taxa of the *Hylopezus/Myrmothera* clade (Fig. 1). Future studies should provide more densely sampled phylogenies of the genera *Grallaricula* and *Grallaria*, therefore allowing for a more accurate positioning of *H. nattereri* in the family phylogeny.

The paraphyly of *M. campanisona* with respect to *M. simplex* supports splitting the former in two separate species, hence recognizing the eastern Amazonian endemic taxon *subcanescens* Todd, 1927, as an independent species, the Tapajos Antpitta *Myrmothera subcanescens* (Krabbe and Schulenberg, 2017). This split is consistent with major vocal differences recognized in the polytypic *M. campanisona* between clade C (to which the name *campanisona* applies) and clades A and B (to which the only name available is *subcanescens;* Krabbe and Schulenberg, 2017; Boesman, 2016).

5. Conclusions

Our analyses provided an additional scenario for the evolution and biological diversification in the Neotropical region. The spatio-temporal pattern recovered herein for the *Hylopezus/Myrmothera* clade may reflect an evolutionary history which has not been influenced solely by strict vicariance due to development of multiple barriers during the Neogene. Instead, clade age and episodes of dispersal have also played an important role in the group's diversification, which did not experience any major rate changes in the last 20 million years (Table 1; Figs. 1 and 3). Therefore, the combination of lineage specific historical and natural history traits along with the continuous formation of barriers throughout the Neotropics can account for the modern diversification of the *Hylopezus/Myrmothera* clade, which stretched from the Pliocene to the Quaternary, when remarkable changes to the Amazon River drainage occurred (Hoorn et al., 2010). This allowed for several episodes of colonization followed by cladogenesis throughout the Amazonian Basin all the way through the Quaternary (Figs. 1 and 3). Our biogeographic inferences recovered a distribution centered in the western Amazonian sedimentary basin, with a later dispersion towards eastern Amazonia during the Late Miocene (Figs. 2 and 3) (Hoorn et al., 2010). However, Amazonian antpittas apparently have strict ecological requirements, and limited ability to colonize new areas, and these facts could explain the relatively few number of extant taxa in the group when compared to other Neotropical lowland lineages of similar age. Finally, our phylogenetic hypotheses also support a new taxonomic classification for the genera *Hylopezus* and *Myrmothera*.

Appendix A

See Figs. A1–A3 and Tables A1–A4.

Acknowledgements

We thank the curators and curatorial assistants of the following collections for allowing us to sequence samples under their care (for acronyms, see text): NMNH, ANSP, INPA, FMNH, LGBM, LGEMA. Field and laboratory work related to this paper were generously funded by CNPq (grants #310593/2009-3; “INCT em Biodiversidade e Uso da Terra da Amazônia” 574008/2008-0; # 563236/2010-8; and # 471342/2011-4) and FAPESPA (ICAAF 023/2011 and 010/2012). Invaluable support was also obtained through a collaborative grant, Dimensions US-Biota-São Paulo: Assembly and evolution of the Amazon biota and its environment: an integrated approach, co-funded by the US National Science Foundation (NSF DEB 1241056), National Aeronautics and Space Administration (NASA), and the Fundação de Amparo à Pesquisa do Estado de São Paulo (FAPESP grant #2012/50260-6). Work by GAB, NA, and AMC at Louisiana State University was supported by NSF grant (DEB-1011435) to GAB. We thank C. Ribas, P. Rêgo, M. Sturaro and P. Peloso, for contributions to earlier versions of the manuscript. L.S.C. was supported by CAPES and FAPESPA fellowships during the study (FAPESPA grant #021/2016). AA is supported by a CNPq research productivity fellowship (#306843/2016-1).

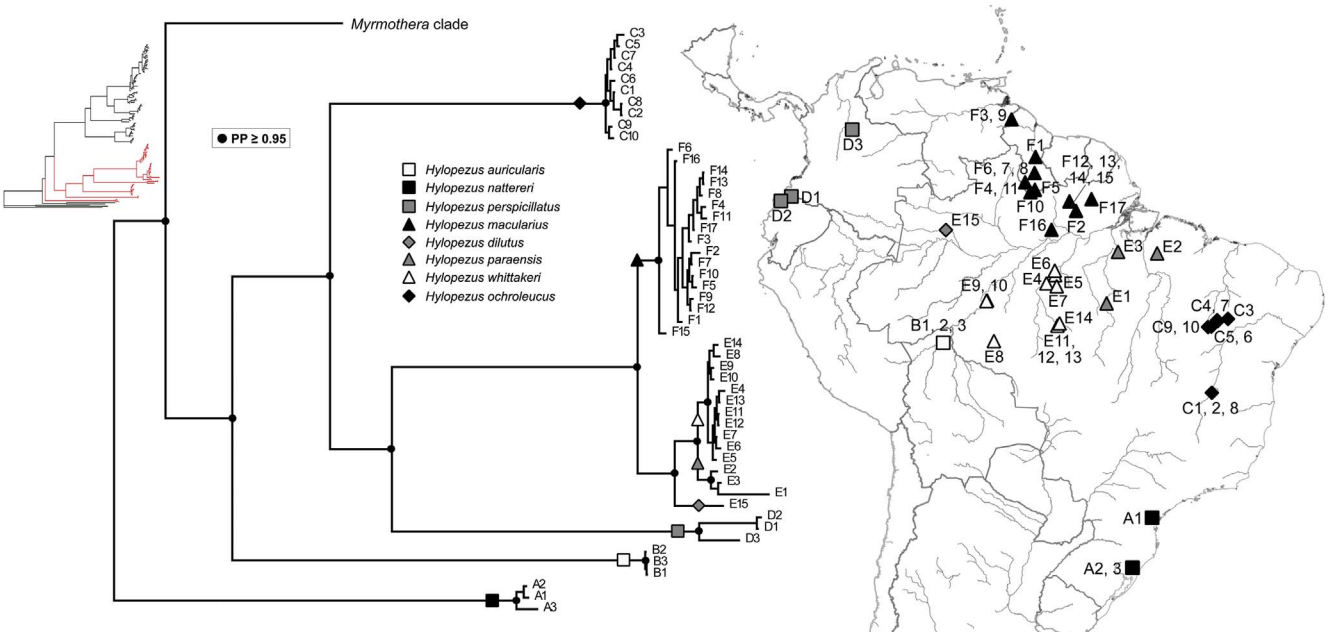

Fig. A1. Multilocus concatenated Bayesian phylogeny of the so-called 'core *Hylopezus*' (see above) based on mtDNA (ND2 and ND3) and nucDNA (TGFB2, MUSK, FGB-I5) genes. Complete phylogeny: top left; nodes and braches in red are those shown here in detail for the 'core *Hylopezus*'. Symbols denote recognized species; for nomenclature details see (Carneiro et al., 2012; Krabbe and Schulenberg, 2003). The map depicts the locations of sampled specimens symbolized and labeled as in the tree and Table A1. Significant nodal Bayesian posterior probabilities (PP) are indicated by black circles. (For interpretation of the references to color in this figure legend, the reader is referred to the web version of this article.)

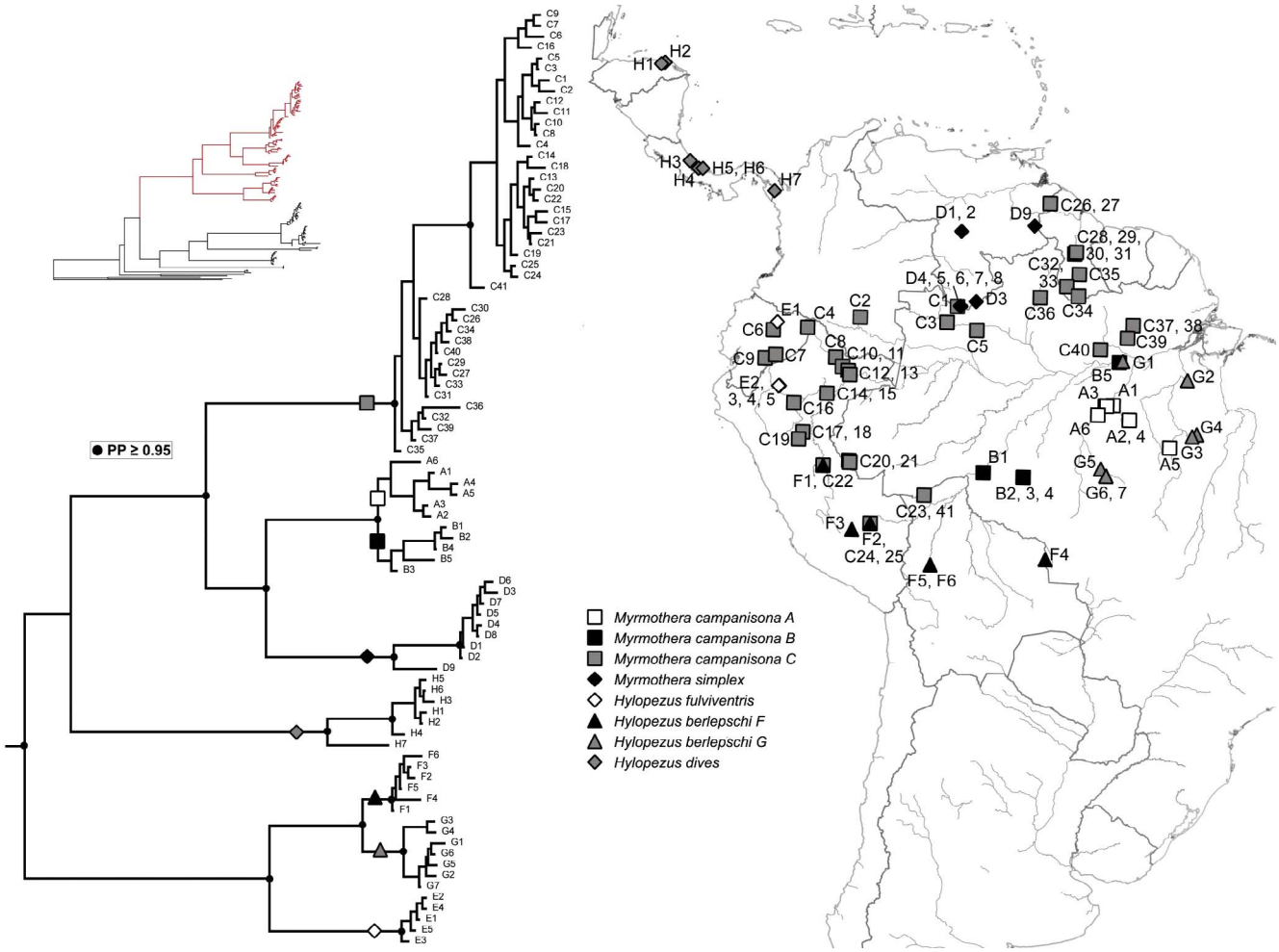

Fig. A2. Multilocus concatenated Bayesian phylogeny of the so-called 'extended *Myrmothera*' clade (see results) based on mtDNA (ND2 and ND3) and nDNA (TGFB2, MUSK, FGB-I5) genes. Complete phylogeny: top left; nodes and braches in red are those shown here in detail for the 'extended *Myrmothera*'. Symbols denote recognized lineages of the five currently recognized species belonging to this clade (Krabbe and Schulenberg, 2003). The map shows the locations of sampled specimens symbolized and labeled as in the tree and Table A1. Significant nodal Bayesian posterior probabilities (PP) are indicated by black circles. (For interpretation of the references to color in this figure legend, the reader is referred to the web version of this article.)

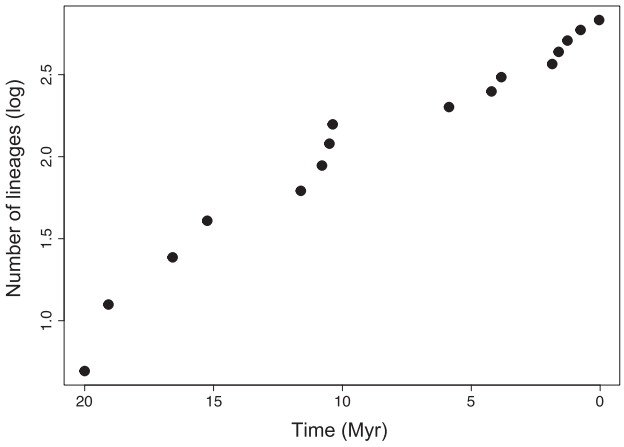

Fig. A3. Lineage through time plot (LTT) of *Grallaricula*, *Hylopezus* and *Myrmothera* inferred from a timetree generated by BEAST based on our multilocus species tree reconstruction.

Table A1
Tissue samples used in this study and their respective tissue collection catalog numbers. Collections: AMNH – American Museum of Natural History, New York; ANSP – Academy of Natural Sciences of Drexler University, Philadelphia; FMNH – Field Museum of Natural History, Chicago; IAvH – Instituto Alexander von Humboldt, Villa de Leyva, Colombia; ICN – Instituto de Ciencias Naturales, Bogotá, Colombia; INPA – Instituto Nacional de Pesquisas da Amazônia, Manaus, Brazil; KU – University of Kansas Natural History Museum, Lawrence; LGEMA – Laboratório de Genética e Evolução Molecular de Aves da Universidade de São Paulo, São Paulo, Brazil; LSUMZ – Louisiana State University Museum of Natural Science, Baton Rouge; MCP – Coleção de Ornitologia do Museu de Ciências e Tecnologia da Pontifícia Universidade Católica do Rio Grande do Sul, Porto Alegre, Brazil; MPEG – Museu Paraense Emílio Goeldi, Belém, Brazil; USNM – United States National Museum, Smithsonian Institution, Washington DC; Taxonomy follows Remsen et al. (2017), except for *H. macularius* complex, which follows Carneiro et al. (2012).

Taxon	Locality	Voucher	Map ID
Myrmothera campanisona	Brazil: Pará; Estern margin Rio Tapajós e direita do Jamanxin SW Itaituba	INPA A-10032	A1
Myrmothera campanisona	Brazil: Pará; Itaituba, margem direita Rio Tapajós, Comunidade Penedo	MPEG 19634	A2
Myrmothera campanisona	Brazil: Pará; Margem direita do Rio Tapajós; 147 km sudoeste de Itaituba	INPA A-11548	A3
Myrmothera campanisona	Brazil: Pará; Altamira, Floresta Nacional de Altamira	MPEG TM008	A4
Myrmothera campanisona	Brazil: Pará; Rio Xingú, margem esquerda, Bom Jardim, Anapú	MPEG BMP075	A5
Myrmothera campanisona	Brazil: Pará; Jacareacanga, margem esquerda Rio Tapajós, Vila Mamãe-anã	MPEG 18604	A6
Myrmothera campanisona	Brazil: Rondônia; Porto Velho; margem direita do Rio Jaci; Três Praias	INPA A-4141	B1
Myrmothera campanisona	Brazil: Rondônia; Cachoeira Nazaré, W bank Rio Jiparaná, 100 m	FMNH 389885	B2
Myrmothera campanisona	Brazil: Rondônia; Cachoeira Nazaré, W bank Rio Jiparaná, 100 m	FMNH 389886	B3
Myrmothera campanisona	Brazil: Rondônia; Cachoeira Nazare, W bank Rio Jiparana, 100 m	FMNH 395993	B4
Myrmothera campanisona	Brazil: Pará; Juruti, Projeto Juruti/Alcoa, Platô Capiranga, trilha 196	MPEG MPDS0961	B5
Myrmothera campanisona	Venezuela: Amazonas; Cerro de la Neblina Base Camp 140 m	LSUMZ B-7563	C1
Myrmothera campanisona	Colombia: Caquetá, Solano, Bombonal, Río Mesay	ICN 32913	C2
Myrmothera campanisona	Brazil: Amazonas; São Gabriel da Cachoeira, PPBIO	MPEG 20648	C3
Myrmothera campanisona	Ecuador: Napo; Zancudo Cocha	ANSP 18324	C4
Myrmothera campanisona	Brazil: Amazonas; 110 km ENE Santa Isabel do Rio Negro	INPA A-1662	C5
Myrmothera campanisona	Ecuador: Napo; Pasohurco; km 57 on Hollín-Loreto Road	ANSP 19457	C6
Myrmothera campanisona	Ecuador: Morona-Santiago; 5 km SW Taisha	ANSP 17546	C7
Myrmothera campanisona	Peru: Loreto; 1 km N Río Napo, 157 km by river NNE Iquitos	LSUMZ B-2756	C8
Myrmothera campanisona	Ecuador: Morona-Santiago; Santiago	ANSP 16450	C9
Myrmothera campanisona	Peru: Loreto; Lower Río Napo region, E. bank Rio Yanayacu, N Iquitos	LSUMZ B-4172	C10
Myrmothera campanisona	Peru: Loreto; Lower Río Napo region, E bank Rio Yanayacu, N Iquitos	LSUMZ B-4346	C11
Myrmothera campanisona	Peru: Loreto; 1 km N Río Napo, 157 km by river NNE Iquitos	LSUMZ B-2867	C12
Myrmothera campanisona	Peru: Loreto; S Río Amazonas, ca 10 km SSW mouth Rio Napo	LSUMZ B-5066	C13
Myrmothera campanisona	Peru: Loreto; S bank Maranon River, Est. Biol. Pithecia.	LSUMZ B-103576	C14
Myrmothera campanisona	Peru: Loreto; S bank Marañón R., Est. Biol. Pithecia	LSUMZ B-3617	C15
Myrmothera campanisona	Peru: Loreto; Ca 7 km S Jeberos	LSUMZ B-42523	C16
Myrmothera campanisona	Peru: Loreto; 79 km WNW Contamana, ca	LSUMZ B-27987	C17
Myrmothera campanisona	Peru: Loreto; 79 km WNW Contamana, ca	LSUMZ B-27991	C18
Myrmothera campanisona	Peru: Loreto; Ca. 86 km SE Juanjui on E bank upper Río Pauya	LSUMZ B-39839	C19
Myrmothera campanisona	Brazil: Acre; Rio Juruá, Marechal Taumaturgo, Nossa Senhora Aparecida	MPEG PNSD337	C20
Myrmothera campanisona	Brazil: Acre; Reserva Extravista Alto Juruá, Rio Tejo,	FMNH 395576	C21
Myrmothera campanisona	Peru: Ucayali; SE slope Cerro Tahuayo, ca 65 km ENE Pucallpa	LSUMZ B-11218	C22
Myrmothera campanisona	Bolivia: Pando; Nicolás Suarez; 12 km by road S of Cobija	LSUMZ B-9600	C23
Myrmothera campanisona	Peru: Madre de Dios; Moskitania, 13.4 km NNW Atalaya, l bank Alto Madre de Dios	FMNH 433462	C24
Myrmothera campanisona	Peru: Madre de Dios; Moskitania, 13.4 km NNW Atalaya, l bank Alto Madre de Dios	FMNH 433464	C25
Myrmothera campanisona	Guyana: Barima-Waini, Baramita; in Former North West Region	USNM 586403	C26
Myrmothera campanisona	Guyama: Barima-Waini, Baramita; in Former North West Region	USNM 621449	C27
Myrmothera campanisona	Guyana: Potaro-Siparuni; Iwokrama Reserve; Kobacalli Landing	ANSP 21242	C28
Myrmothera campanisona	Guyana: Potaro-Siparuni; Iwokrama Reserve; ca. 41 road km, SW Kurupukari	ANSP 21109	C29
Myrmothera campanisona	Guyana: Potaro-Siparuni; Iwokrama Reserve; ca. 6–8 road mi. SW Kurupukari	ANSP 22305	C30
Myrmothera campanisona	Guyana: Upper Takutu – Upper Essequibo; lower Rewa River	USNM 637266	C31
Myrmothera campanisona	Guyana: Parabara Savannah	USNM 622361	C32
Myrmothera campanisona	Guyana: Parabara Savannah	KU B-12708	C33

(*continued on next page*)

Table A1 (*continued*)

Taxon	Locality	Voucher	Map ID
Myrmothera campanisona	Guyana: Gunn'S Landing, West Bank Upper Essequibo River	USNM 616546	C34
Myrmothera campanisona	Guyana: Upper Essequibo River	USNM 625540	C35
Myrmothera campanisona	Brazil: Roraima; Parque Nacional Viruá, margem esquerda do Rio Branco	INPA A-1726	C36
Myrmothera campanisona	Brazil: Pará; Alenquer, ESEC Grão-Pará	MPEG CN418	C37
Myrmothera campanisona	Brazil: Pará; Alenquer, ESEC Grão-Pará	MPEG CN509	C38
Myrmothera campanisona	Brazil: Pará: Óbidos, Flota do Trombetas	MPEG CN341	C39
Myrmothera campanisona	Brazil: Pará; FLOTA de Faro, ca 70 km NW de Faro	MPEG CN150	C40
Myrmothera campanisona	Bolivia: Pando, Nicolás Suarez; 12 km by road S of Cobija	LSUMZ B-8955	C41
Myrmothera simplex	Venezuela: Amazonas; Cerro Yavi	AMNH 213312	D1
Myrmothera simplex	Venezuela: Amazonas; Cerro Yavi	AMNH 213320	D2
Myrmothera simplex	Venezuela: Amazonas; Sierra de Tapirapeco; Cerro Tamacuari; 1270 m	AMNH GFB2136	D3
Myrmothera simplex	Venezuela: Amazonas; Pico Cardonas; Elev. 1250 M Rainforest, Valley N. Base	AMNH RWD17126	D4
Myrmothera simplex	Venezuela: Amazonas; Cerro de la Neblina; Camp VII 1800–1900 M	AMNH GFB1440	D5
Myrmothera simplex	Venezuela, Amazonas; Cerro de la Neblina; Camp VII 1800 M	LSUMZ B-7407	D6
Myrmothera simplex	Venezuela, Amazonas; Cerro de la Neblina; Camp VII 1800 M	LSUMZ B-7408	D7
Myrmothera simplex	Venezuela, Amazonas; Cerro de la Neblina; Camp VII 1800 M	LSUMZ B-7468	D8
Myrmothera simplex	Venezuela: Bolívar; La Escalera, KM 122 on El dorado-ST. Eleanea Road	AMNH RDP301	E1
Hylopezus fulviventris	Ecuador: Napo; 20 road km W of Coca; south bank Rio Payamino	ANSP 18744	F1
Hylopezus fulviventris	Peru, Loreto; Ca 54 km NNW mouth Río Morona on east bank	LSUMZ B-43007	F2
Hylopezus fulviventris	Peru, Loreto; Ca 54 km NNW mouth Río Morona on west bank	LSUMZ B-43008	F3
Hylopezus nattereri	Brazil: Paraná; Quatro Barras, Corvo	MPEG CMN024	A1
Hylopezus nattereri	Brazil: Rio Grande do Sul; Condominio Alpes- São Francisco de Paula	MCP 3057	A2
Hylopezus nattereri	Brazil: Rio Grande do Sul; CPCN Pró-Mata, São Francisco de Paula	MCP 3345	A3
Hylopezus auricularis	Bolivia: El Beni; Hamburgo, 1 km W Riberalta	FMNH 391156	B1
Hylopezus auricularis	Bolivia: El Beni; Hamburgo, 1 km W Riberalta	FMNH 391157	B2
Hylopezus auricularis	Bolivia: El Beni; Hamburgo, 1 km W Riberalta	FMNH 391158	B3
Hylopezus ochroleucus	Brazil: Minas Gerais; Mocambinho, Jaíba	LGEMA 2318	C1
Hylopezus ochroleucus	Brazil: Minas Gerais; Mocambinho, Jaíba	LGEMA 2036	C2
Hylopezus ochroleucus	Brazil: Piauí, São Raimundo Nonato, PN Serra da Capivara, Serra Vermelha	MPEG 18943	C3
Hylopezus ochroleucus	Brazil: Piauí, Caracol, PN Serra das Confusões, Projeto Cajugaia	MPEG 18962	C4
Hylopezus ochroleucus	Brazil: Piauí, Cristino Castro, PN Serra das Confusões, Baixo Japecanga	MPEG 18984	C5
Hylopezus ochroleucus	Brazil: Piauí, Cristino Castro, PN Serra das Confusões, Baixo Japecanga	MPEG 18985	C6
Hylopezus ochroleucus	Brazil: Piauí, Caracol, P. N. Serra das Confusões, Centro de Visitantes	MPEG 20156	C7
Hylopezus ochroleucus	Brazil: Minas Gerais: Mocambinho, Jaiba	MCP JB134	C8
Hylopezus ochroleucus	Brazil: Morro Cabeça no Tempo, Serra Vermelha	MPEG SRV104	C9
Hylopezus ochroleucus	Brazil: Curimatá, Serra Vermelha	MPEG SRV004	C10
Hylopezus perspicilatus	Ecuador: Esmeraldas; 20 road km NNW Alto Tambo	ANSP – 17269	D1
Hylopezus perspicilatus	Ecuador: Esmeraldas; 30 km S Chontaduro; W bank Rio Verde	ANSP – 19055	D2
Hylopezus perspicillatus	Colombia: Santander; Flores Blancas	ICN 36133	D3
Hylopezus paraensis	Brazil: Pará; Rio Xingú, margem direita, Caracol, Anapu	MPEG BMP074	E1
Hylopezus paraensis	Brazil: Pará; Paragominas, Fazenda Rio Capim, CIKEL	MPEG FRC078	E2
Hylopezus paraensis	Brazil: Pará; Rio Xingú, margem direita, Senador José Porfírio	MPEG UHE388	E3
Hylopezus whittakeri	Brazil: Pará; Jacareacanga, margem direita Rio Tapajós, Comunidade São Martim	MPEG 18511	E4
Hylopezus whittakeri	Brazil: Pará; Itaituba, leste do Tapajós, Rio Ratão	MPEG 18776	E5
Hylopezus whittakeri	Brazil: Pará; Itaituba, leste do Tapajós, Jatobá	MPEG 18803	E6
Hylopezus whittakeri	Brazil: Pará; Jacareacanga, margem direita Rio Crepori	MPEG 19599	E7
Hylopezus whittakeri	Brazil: Rondônia; Cachoeira Nazaré, W bank Rio Jiparana	FMNH 389869	E8
Hylopezus whittakeri	Brazil: Amazonas; Barra de São Manoel	LSUMZ B-78245	E9
Hylopezus whittakeri	Brazil: Amazonas; Humaitá, T. Indígena Parintintin, Aldeia Traíra-Chororó	MPEG MPDS719	E10
Hylopezus whittakeri	Brazil: Mato Grosso; Paranaíta, margem direita Rio Paranaíta, Fazenda Rio Paranaíta	MPEG TLP178	E11
Hylopezus whittakeri	Brazil: Mato Grosso; Paranaíta, margem direita Rio Paranaíta, Fazenda Rio Paranaíta	MPEG TLP(A)179	E12
Hylopezus whittakeri	Brazil: Mato Grosso; Paranaíta, margem esquerda Rio Paranaíta, Fazenda Aliança	MPEG TLP(A)404	E13
Hylopezus whittakeri	Brazil: Mato Grosso; Paranaíta, Rio Teles Pires, margem direita	MPEG TLP(C)095	E14
Hylopezus dilutus	Brazil: Amazonas; Maraã, Lago Cumapi	MPEG JAP636	E15
Hylopezus macularius	Guyana: Iwokrama Reserve; Kobacalli Landing	ANSP – 21224	F1
Hylopezus macularius	Brazil: Pará; Alenquer, ESEC Grão	MPEG 66053	F2
Hylopezus macularius	Guyana: Barima-Waini; Baramita, In Former North West Region	USNM 586404	F3
Hylopezus macularius	Guyana: Parabara Savannah	USNM 616605	F4
Hylopezus fulviventris	Peru, Loreto; Ca 54 km NNW mouth Río Morona on west bank	LSUMZ B-43009	F4
Hylopezus macularius	Guyana: Gunn'S Landing, 10 km SSE	USNM 625539	F5
Hylopezus fulviventris	Peru: Loreto; Ca 54 km NNW mouth of Río Morona, on east bank	LSUMZ B-42791	F5
Hylopezus macularius	Guyana: Upper Takutu – Upper Essequibo; Upper Rewa River	USNM 637111	F6
Hylopezus macularius	Guyana: Upper Takutu – Upper Essequibo; Upper Rewa River	USNM 637226	F7
Hylopezus macularius	Guyana: Upper Takutu – Upper Essequibo; lower Rewa River	USNM 637238	F8
Hylopezus macularius	Guyana: Northwest District; Baramita	KU B-9754	F9
Hylopezus macularius	Guyana: Acari Mountains, N side	KU B-10765	F10
Hylopezus macularius	Guyana: Parabara Savannah	KU B-12706	F11
Hylopezus macularius	Brazil: Pará; Óbidos, ESEC Grão-Pará	MPEG CN1274	F12
Hylopezus macularius	Brazil: Pará; Óbidos, ESEC Grão-Pará	MPEG CN1328	F13
Hylopezus macularius	Brazil: Pará; Óbidos, ESEC Grão-Pará	MPEG CN1329	F14
Hylopezus macularius	Brazil: Pará; Óbidos, ESEC Grão-Pará	MPEG CN1332	F15
Hylopezus macularius	FLOTA de Faro, ca 70 km NW de Faro	MPEG CN143	F16
Hylopezus macularius	Brazil: Pará; Almeirim, REBIO Maicuru	MPEG CN901	F17
Hylopezus berlepschi	Peru: Ucayali; SE slope Cerro Tahuayo, ca km ENE Pucallpa	LSUMZ B-11146	G1
Hylopezus berlepschi	Peru: Madre de Dios; Moskitania, 13.4 km NNW of Atalaya	FMNH 433523	G2

(*continued on next page*)

Table A1 (*continued*)

Taxon	Locality	Voucher	Map ID
Hylopezus berlepschi	Peru: Madre de Dios; Hacienda Amazonia	FMNH 322345	G3
Hylopezus berlepschi	Bolivia: Santa Cruz; Velasco; Parque Nacional Noel Keonpff Mercado	LSUMZ B-18312	G4
Hylopezus berlepschi	Bolivia: La Paz; Río Beni, ca 20 km by river N. Puerto Linares	LSUMZ B-1057	G5
Hylopezus berlepschi	Bolivia: La Paz; Río Beni, ca 20 km by river N. Puerto Linares	LSUMZ B-1072	G6
Hylopezus berlepschi	Brazil: Amazonas; Santarém, Retiro	MPEG PIME022	H1
Hylopezus berlepschi	Brazil: Pará; Rio Xingu, Altamira, Ilha da Taboca, UHE Belo Monte	MPEG UHE046	H2
Hylopezus berlepschi	Brazil: Pará, Município de Ourilândia do Norte	MPEG DPN158	H3
Hylopezus berlepschi	Brazil: Rio Xingu, margem direita, Itapuama	MPEG BMP024	H4
Hylopezus berlepschi	Brazil: Pará; E. bank R. Teles Pires, 4 km from the mouth of the Rio Sao benedito	LSUMZ B-35407	H5
Hylopezus berlepschi	Brazil: Mato Grosso; Paranaíta, Rio Teles Pires, margem esquerda	MPEG TLP(A)272	H6
Hylopezus berlepschi	Brazil: Mato Grosso; Paranaíta, margem direita Rio Paranaíta, Fazenda Paranaíta	MPEG TLP(A)386	H7
Hylopezus dives	Honduras, Gracias a Dios; Las Marías, on Río Platano, 25 km S Caribbean Sea	LSUMZ B-26087	I1
Hylopezus dives	Honduras, Gracias a Dios; Las Marías, on Río Platano, 25 km S Caribbean Sea	LSUMZ B-26086	I2
Hylopezus dives	Costa Rica: Limón; Limón, Reserva Biológica Hitoy Cerere	LSUMZ B-82039	I3
Hylopezus dives	Panama: Bocas del Toro; Río Changuinola Arriba, W bank	LSUMZ B-46450	I4
Hylopezus dives	Panamá: Bocas Del Toro, Tierra Oscura	USNM 606954	I5
Hylopezus dives	Panamá: Bocas Del Toro, Tierra Oscura	USNM 612384	I6
Hylopezus dives	Panama: Darién; Cana on E slope Cerro Pirre	LSUMZ B-2283	I7
Grallaricula nana	Colombia: Norte de Santander; PNN Tamá, Orocué	IAvH BT-11540	–
Grallaricula flavirostris	Colombia: Antioquia; Anorí, Alto El Chaquiral	IAvH BT-4774	–
Grallaria rufula	Peru: Cajamarca; Quebrada Lanchal, ca 8 km ESE Sallique	LSUMZ B-32257	–
Grallaria ruficapilla	Colombia: Caldas; Aranzazu, Hacienda Termópilas	IAvH BT-1666	–
Grallaria guatimalensis	Costa Rica: Puntarenas; Monteverde, Cerro Plano	LSUMZ B-82156	–

Table A2
List of primers used in the study.

Gene	Annealing Temp.	Primmer	Reference
NADH dehydrogenase subunits 2 (ND2, 1041 bps)	56 °C	L5215H6313	Hackett (1996) Sorenson et al. (1999)
NADH dehydrogenase subunits 3 (ND3, 351 bps)	56 °C	L5215H6313	Hackett (1996) Sorenson et al. (1999)
Transforming growth factor beta 2 intron 5 (TGFB2, 625 bps)	60 °C	L6625/H7005	Hafner et al. (1994)
Beta-fibrinogen intron 5 (FGB-I5, 549 bps)	63 °C	FIB5L/FIB5H	Driskell and Christidis (2004)
3rd intron of the Z-linked muscle-specific kinase (MUSK, 582 bp)	63 °C	MUSK-F/MUSK-R	Kimball et al. (2009)

Table A3
Best partitioning scheme and the best-fit models selected for each partition evaluated in PartitionFinder by the Bayesian Information Criterion (BIC).

Subset	Best model	Subset partitions	Subset sites
1	TrN + I + G	ND2_pos1, ND2_pos2, ND3_pos1	1-1039\3, 2-1040\3, 1042-1390\3
2	GTR + I + G	ND2_pos3, ND3_pos3	3-1041\3, 1044-1392\3
3	GTR + I + G	BF5, MUSK, ND3_pos2, TGFB2	1043-1391\3, 1393-1974, 1975-2599, 2600-3148

Table A4
Biogeographic regions used in the BioGeoBears analyses.

And: Andes. includes Northern and Central Andes Cordillera
BSh: Brazilian Shield. We combined the Belém, Xingu, Tapajós and Madeira centers of endemism (da Silva et al., 2005)
Caa: Caatinga. Xeric shrubland forest endemic from Northeastern Brazil, Adapted Morrone (2014)
CAm: Central America. includes Caribbean slope from eastern Honduras, western coast of Costa Rica and Panamá
Cho: Chocó. Pacific coast of northern Ecuador and Colombia
GSh: Guiana Shield. includes north of the Amazon River, east of the Rio Branco, and east of the Orinoco River (da Silva et al., 2005; Morrone, 2014)
SAF: Atlantic Forest of southeastern South America. includes only the southern portion of the Atlantic Forest, Adapted from Morrone (2014)
SBa: Amazon Sedimentary basin. includes Rondônia, Imeri, Napo and Negro centers of (Borges and Da Silva, 2012; da Silva et al., 2005) i.e., the areas west of the Branco and Madeira rivers in Amazonia
Tep: Tepuis. Northwestern South America, on the Guianan Shield, between Venezuela, Colombia, Guyana, Suriname and northern Brazil, where there are sandy plateaus or Tepuis higher than 2000 m altitude (Morrone, 2014)

Appendix B. Supplementary material

Supplementary data associated with this article can be found, in the online version, at http://dx.doi.org/10.1016/j.ympev.2017.11.019.

References

Aleixo, A., 2004. Historical diversification of a terra-firme forest bird superspecies: a phylogeographic perspective on the role of different hypotheses of Amazonian diversification. Evolution 58, 1303–1317. http://dx.doi.org/10.1554/03-158.

Ames, P.L., 1971. The morphology of the syrinx in passerine birds. Peabody Museum Bull. 37, 241.

Antonelli, A., Sanmartín, I., 2011. Why are there so many plant species in the Neotropics? Taxon 60, 403–414. http://dx.doi.org/10.2307/41317138.

Baker, P.A., Fritz, S.C., 2015. Nature and causes of Quaternary climate variation of tropical South America 124.

Batalha-Filho, H., Pessoa, R.O., Fabre, P.H., Fjeldså, J., Irestedt, M., Ericson, P.G.P., Silveira, L.F., Miyaki, C.Y., 2014. Phylogeny and historical biogeography of gnateaters (Passeriformes, Conopophagidae) in the South America forests. Mol. Phylogenet. Evol. 79, 422–432. http://dx.doi.org/10.1016/j.ympev.2014.06.025.

Boesman, P., 2016. Notes on the vocalizations of Thrush-like Antpitta (Myrmothera campanisona). HBW Alive Ornithological Note 74. In: Handbook of the Birds of the World Alive. Lynx Edicions, Barcelona. (retrieved from http://www.hbw.com/node/931962 on 18 May 2016).

Borges, S.H., Da Silva, J.M.C., 2012. A new area of endemism for Amazonian birds in the Rio Negro Basin. Wilson J. Ornithol. 124, 15–23. http://dx.doi.org/10.1676/07-103.1.

Brumfield, R.T., Edwards, S.V., 2007. Evolution into and out of the Andes: a baysian analysis of historical diversification in Thamnophilus antshrikes. Evolution (N. Y). 346–367. http://dx.doi.org/10.1111/j.1558-5646.2007.00039.x.

Brumfield, R.T., Tello, J.G., Cheviron, Z.A., Carling, M.D., Crochet, N., Rosenberg, K.V., 2007. Phylogenetic conservatism and antiquity of a tropical specialization: army-ant-following in the typical antbirds (Thamnophilidae). Mol. Phylogenet. Evol. 45, 1–13. http://dx.doi.org/10.1016/j.ympev.2007.07.019.

Bryson, R.W., Chaves, J., Smith, B.T., Miller, M.J., Winker, K., Pérez-Emán, J.L., Klicka, J., 2014. Diversification across the New World within the "blue" cardinalids (Aves: Cardinalidae). J. Biogeogr. 41, 587–599. http://dx.doi.org/10.1111/jbi.12218.

Burney, C.W., Brumfield, R.T., 2009. Ecology predicts levels of genetic differentiation in neotropical birds. Am. Nat. 174, 358–368. http://dx.doi.org/10.1086/603613.

Campbell, K.E., Frailey, C.D., Romero-Pittman, L., 2006. The Pan-Amazonian Ucayali Peneplain, late Neogene sedimentation in Amazonia, and the birth of the modern Amazon River system. Palaeogeogr. Palaeoclimatol. Palaeoecol. 239, 166–219. http://dx.doi.org/10.1016/j.palaeo.2006.01.020.

Carneiro, L.S., Gonzaga, L.P., Rêgo, P.S., Sampaio, I., Schneider, H., Aleixo, A., 2012. Systematic revision of the spotted anppitta (Grallariidae: Hylopezus macularius), with description of a new species from Brazilian Amazonia. Auk 129, 338–351.

Castroviejo-Fisher, S., Guayasamin, J.M., Gonzalez-Voyer, A., Vilà, C., 2014. Neotropical diversification seen through glassfrogs. J. Biogeogr. 41, 66–80. http://dx.doi.org/10.1111/jbi.12208.

Chaves, J.A., Weir, J.T., Smith, T.B., 2011. Diversification in Adelomyia hummingbirds follows Andean uplift. Mol. Ecol. 20, 4564–4576. http://dx.doi.org/10.1111/j.1365-294X.2011.05304.x.

Clegg, S.M., Phillimore, A.B., 2010. The influence of gene flow and drift on genetic and phenotypic divergence in two species of Zosterops in Vanuatu. Philos. Trans. R. Soc. B Biol. Sci. 365, 1077–1092. http://dx.doi.org/10.1098/rstb.2009.0281.

D'Horta, F.M., Cuervo, A.M., Ribas, C.C., Brumfield, R.T., Miyaki, C.Y., 2012. Phylogeny and comparative phylogeography of Sclerurus (Aves: Furnariidae) reveal constant and cryptic diversification in an old radiation of rain forest understorey specialists. J. Biogeogr. 40, 37–49. http://dx.doi.org/10.1111/j.1365-2699.2012.02760.x.

da Silva, J.M.C., Rylands, A.B., Fonseca, G.A.B., 2005. The fate of the Amazonian areas of endemism. Conserv. Biol. 19, 689–694.

De-silva, D.L., Elias, M., Willmott, K., Mallet, J., Day, J.J., 2016. Diversification of clearwing butterflies with the rise of the Andes. J. Biogeogr. 43, 44–58. http://dx.doi.org/10.1111/jbi.12611.

Derryberry, E.P., Claramunt, S., Derryberry, G., Chesser, R.T., Cracraft, J., Aleixo, A., Pérez-Emán, J., Remsen, J.V., Brumfield, R.T., 2011. Lineage diversification and morphological evolution in a large-scale continental radiation: the neotropical ovenbirds and woodcreepers (aves: furnariidae). Evolution (N. Y). 65, 2973–2986. http://dx.doi.org/10.1111/j.1558-5646.2011.01374.x.

Driskell, A.C., Christidis, L., 2004. Phylogeny and evolution of the Australo-Papuan honeyeaters (Passeriformes, Meliphagidae). Mol. Phylogenet. Evol. 31, 943–960. http://dx.doi.org/10.1016/j.ympev.2003.10.017.

Drummond, A.J., Ho, S.Y.W., Phillips, M.J., Rambaut, A., 2006. Relaxed phylogenetics and dating with confidence. PLoS Biol. 4, 699–710. http://dx.doi.org/10.1371/journal.pbio.0040088.

Drummond, A.J., Rambaut, A., 2007. BEAST: Bayesian evolutionary analysis by sampling trees. BMC Evol. Biol. 7, 214.

Drummond, A.J., Suchard, M.A., Xie, D., Rambaut A., 2012. Bayesian phylogenetics with BEAUti and the BEAST 1.7. Mol. Biol. Evol. 29, 1969–1973.

Edwards, S., Beerli, P., 2000. Perspective: gene divergence, population divergence, and the variance in coalescence time in phylogeographic studies. Evolution (N. Y). 54, 1839–1854. http://dx.doi.org/10.1111/j.0014-3820.2000.tb01231.x.

Ellegren, H., 2007. Molecular evolutionary genomics of birds. Cytogenet. Genome Res. 117, 120–130.

Fabre, P.H., Galewski, T., Tilak, M.K., Douzery, E.J.P., 2013. Diversification of South American spiny rats (Echimyidae): a multigene phylogenetic approach. Zool. Scr. 42, 117–134. http://dx.doi.org/10.1111/j.1463-6409.2012.00572.x.

Fernandes, A.M., Wink, M., Sardelli, C.H., Aleixo, A., 2014. Multiple speciation across the Andes and throughout Amazonia: the case of the spot-backed antbird species complex (Hylophylax naevius/Hylophylax naevioides). J. Biogeogr. 41, 1094–1104. http://dx.doi.org/10.1111/jbi.12277.

Figueiredo, J., Hoorn, C., van der Ven, P., Soares, E., 2009. Late Miocene onset of the Amazon River and the Amazon deep-sea fan: evidence from the Foz do Amazonas Basin. Geology 37, 619–622. http://dx.doi.org/10.1130/G25567A.1.

Fouquet, A., Loebmann, D., Castroviejo-Fisher, S., Padial, J.M., Orrico, V.G.D., Lyra, M.L., Roberto, I.J., Kok, P.J.R., Haddad, C.F.B., Rodrigues, M.T., 2012. From Amazonia: to the Atlantic forest: molecular phylogeny of Phyzelaphryninae frogs reveals unexpected diversity and a striking biogeographic pattern emphasizing conservation challenges. Mol. Phylogenet. Evol. 65, 547–561.

Galewski, T., Mauffrey, J.F., Leite, Y.L.R., Patton, J.L., Douzery, E.J.P., 2005. Ecomorphological diversification among South American spiny rats (Rodentia; Echimyidae): a phylogenetic and chronological approach. Mol. Phylogenet. Evol. 34, 601–615. http://dx.doi.org/10.1016/j.ympev.2004.11.015.

Galvão, A., Gonzaga, L.P., 2011. Morphological support for placement of the Wing-banded Antbird Myrmornis torquata in the Thamnophilidae (Passeriformes: Furnariides). Zootaxa 67, 37–67.

Garzione, C.N., Hoke, G.D., Libarkin, J.C., Withers, S., MacFadden, B., Eiler, J., Ghosh, P., Mulch, A., 2008. Rise of the Andes. Science 320, 1304–1307. http://dx.doi.org/10.1126/science.1148615.

Giehl, E.L.H., Jarenkow, J.A., 2012. Niche conservatism and the differences in species richness at the transition of tropical and subtropical climates in South America. Ecography (Cop.) 35, 933–943. http://dx.doi.org/10.1111/j.1600-0587.2011.07430.x.

Gregory-Wodzicki, K.M., 2000. Uplift history of the Central and Northern Andes: a review. Geol. Soc. Am. Bull. 112, 1091–1105. http://dx.doi.org/10.1130/0016-7606(2000) 112<1091:uhotca>2.0.co;2.

Hackett, S.J., 1996. Molecular phylogenetics and biogeography of tanagers in the genus Ramphocelus (Aves). Mol. Phylogenet. Evol. 5, 368–382. http://dx.doi.org/10.1006/mpev.1996.0032.

Haffer, J., 1974. Avian Speciation in Tropical South America, Publicatio. ed, Avian Speciation in Tropical South America.

Hafner, M.S., Sudman, P.D., Villablanca, F.X., Spradling, T.A., Demastes, J.W., Nadler, S.A., 1994. Disparate rates of molecular evolution in cospeciating host and parasites. Science (80-.).

Harmon, L.J., Weir, J.T., Brock, C.D., Glor, R.E., Challenger, W., 2008. GEIGER: Investigating evolutionary radiations. Bioinformatics 24, 129–131. http://dx.doi.org/10.1093/bioinformatics/btm538.

Heled, J., Drummond, A.J., 2010. Bayesian inference of species trees from multilocus data. Mol. Biol. Evol. 27, 570–580. http://dx.doi.org/10.1093/molbev/msp274.

Hoorn, C., Mosbrugger, V., Mulch, A., Antonelli, A., 2013. Biodiversity from mountain building. Nat. Geosci. 6, 154. http://dx.doi.org/10.1038/ngeo1742.

Hoorn, C., Wesselingh, F.P., ter Steege, H., Bermudez, M.A., Mora, A., Sevink, J., Sanmartin, I., Sanchez-Meseguer, A., Anderson, C.L., Figueiredo, J.P., Jaramillo, C., Riff, D., Negri, F.R., Hooghiemstra, H., Lundberg, J., Stadler, T., Sarkinen, T., Antonelli, A., 2010. Amazonia through time: Andean uplift, climate change, landscape evolution, and biodiversity. Science (80-.). 330, 927–931. http://dx.doi.org/10.1126/science.1194585.

Huelsenbeck, J., Rannala, B., 2004. Frequentist properties of Bayesian posterior probabilities of phylogenetic trees under simple and complex substitution models. Syst. Biol. 53, 904–913. http://dx.doi.org/10.1080/10635150490522629.

Insel, N., Poulsen, C.J., Ehlers, T.A., 2009. Influence of the Andes Mountains on South American moisture transport, convection, and precipitation. Clim. Dyn. 35, 1477–1492. http://dx.doi.org/10.1007/s00382-009-0637-1.

Insel, N., Poulsen, C.J., Ehlers, T.A., Sturm, C., 2012. Response of meteoric? ^{18}O to surface uplift – implications for Cenozoic Andean Plateau growth. Earth Planet. Sci. Lett. 317–318, 262–272. http://dx.doi.org/10.1016/j.epsl.2011.11.039.

Jaramillo, C., Romero, I., Apolito, C.D., Bayona, G., Duarte, E., Louwye, S., Escobar, J., Luque, J., Carrillo-briceño, J.D., Zapata, V., Mora, A., Schouten, S., Zavada, M., Harrington, G., Ortiz, J., Wesselingh, F.P., 2017. Miocene flooding events of western Amazonia. Sci. Adv. 3, 1–11.

Katoh, K., Misawa, K., Kuma, K., Miyata, T., 2002. MAFFT: a novel method for rapid multiple sequence alignment based on fast Fourier transform. Nucleic Acids Res. 30, 3059–3066. http://dx.doi.org/10.1093/nar/gkf436.

Kearse, M., Moir, R., Wilson, A., Stones-Havas, S., Cheung, M., Sturrock, S., Buxton, S., Cooper, A., Markowitz, S., Duran, C., Thierer, T., Ashton, B., Meintjes, P., Drummond, A., 2012. Geneious Basic: an integrated and extendable desktop software platform for the organization and analysis of sequence data. Bioinformatics 28, 1647–1649. http://dx.doi.org/10.1093/bioinformatics/bts199.

Kimball, R.T., Braun, E.L., Barker, F.K., Bowie, R.C.K., Braun, M.J., Chojnowski, J.L., Hackett, S.J., Han, K.L., Harshman, J., Heimer-Torres, V., Holznagel, W., Huddleston, C.J., Marks, B.D., Miglia, K.J., Moore, W.S., Reddy, S., Sheldon, F.H., Smith, J.V., Witt, C.C., Yuri, T., 2009. A well-tested set of primers to amplify regions spread across

the avian genome. Mol. Phylogenet. Evol. 50, 654–660. http://dx.doi.org/10.1016/j.ympev.2008.11.018.
Krabbe, N.K., Schulenberg, T.S., 2003. Family Formicariidae (Ground-Antbirds). In: del Hoyo, J., Elliott, A., Christie, D. (Eds.), In: Handbook of the Birds of the World. Barcelona, pp. 682–731.
Krabbe, N.K., Schulenberg, T.S., 2017. Thrush-like Antpitta (Myrmothera campanisona). In: del Hoyo, J., Elliott, A., Sargatal, J., Christie, D.A. & de Juana, E. (Eds.). Handbook of the Birds of the World Alive. Lynx Edicions, Barcelona. (retrieved from http://www.hbw.com/node/56879 on 14 October 2017).
Lanfear, R., Calcott, B., Ho, S.Y.W., Guindon, S., 2012. PartitionFinder: combined selection of partitioning schemes and substitution models for phylogenetic analyses. Mol. Biol. Evol. 29, 1695–1701.
Latrubesse, E.M., Cozzuol, M., da Silva-Caminha, S.a.F., Rigsby, C.a., Absy, M.L., Jaramillo, C., 2010. The Late Miocene paleogeography of the Amazon Basin and the evolution of the Amazon River system. Earth-Science Rev. 99, 99–124. http://dx.doi.org/10.1016/j.earscirev.2010.02.005.
Lerner, H.R.L., Meyer, M., James, H.F., Hofreiter, M., Fleischer, R.C., 2011. Report multilocus resolution of phylogeny and timescale in the extant adaptive radiation of Hawaiian honeycreepers. Curr. Biol. 21, 1838–1844. http://dx.doi.org/10.1016/j.cub.2011.09.039.
Lima, M.G.M., Buckner, J.C., Queiroz, H., Chiou, K.L., Fiore, A. Di, Alfaro, M.E., Alfaro, J.W.L., 2017. Capuchin monkey biogeography: understanding Sapajus Pleistocene range expansion and the current sympatry between Cebus and Sapajus. J. Biogeogr. 1–11. http://dx.doi.org/10.1111/jbi.12945.
Lowery, G.H., O'Neil, P.O., 1969. A new species of antpitta a from Peru and a revision of the subfamily Grallariinae. Auk 86, 1–12.
Matzke, N.J., 2014. Model selection in historical biogeography reveals that founder-event speciation is a crucial process in island clades. Syst. Biol. 63, 951–970. http://dx.doi.org/10.1093/sysbio/syu056.
Matzke, N.J., 2013. Probabilistic historical biogeography: new models for founder-event speciation, imperfect detection, and fossils allow improved accuracy and model-testing. Front. Biogeogr. 5, 242–248.
Miller, M.A., Pfeiffer, W., Schwartz, T., 2010. Creating the CIPRES Science Gateway for inference of large phylogenetic trees. 2010 Gatew. Comput. Environ. Work. GCE 2010. doi: 10.1109/GCE.2010.5676129.
Minin, V., Abdo, Z., Joyce, P., Sullivan, J., 2003. Performance-based selection of likelihood models for phylogeny estimation 52, 674–683. http://dx.doi.org/10.1080/10635150390235494.
Moore, B.R., Donoghue, M.J., 2007. Correlates of diversification in the plant clade dipsacales: geographic movement and evolutionary innovations. Am. Nat. 170, S28–S55.
Morrone, J.J., 2014. Biogeographical regionalisation of the Neotropical region. Zootaxa 3782, 1–110.
Moyle, R.G., Chesser, R.T., Brumfield, R.T., Tello, J.G., Marchese, D.J., Cracraft, J., 2009a. Phylogeny and phylogenetic classification of the antbirds, ovenbirds, woodcreepers, and allies (Aves: Passeriformes: infraorder Furnariides). Cladistics 25, 1–20.
Moyle, R.G., Filardi, C.E., Smith, C.E., Diamond, J., 2009b. Explosive Pleistocene diversification and hemispheric expansion of a "'great speciator'". PNAS 106, 1863–1868.
Nylander, J.A.A., Wilgenbusch, J.C., Warren, D.L., Swofford, D.L., 2008. AWTY (are we there yet): a system for graphical exploration of MCMC convergence in Bayesian phylogenetics. Bioinformatics 24, 581–583.
Ohlson, J., Irestedt, M., Ericson, P.G.P., Fjeldså, J., 2013. Phylogeny and classification of the New World suboscines (Aves, Passeriformes) 3613, 1–35.
Paradis, E., Claude, J., Strimmer, K., 2004. APE: analyses of phylogenetics and evolution in R language. Bioinformatics 20, 289–290. http://dx.doi.org/10.1093/bioinformatics/btg412.
Patel, S., Weckstein, J.D., Patané, J.S.L., Bates, J.M., Aleixo, A., 2011. Temporal and spatial diversification of *Pteroglossus* Aracaris (Aves Ramphastidae) in the Neotropics: constant rate of diversification does not support an increase in radiation during the Pleistocene. Mol. Phylogenet. Evol. 58, 105–115. http://dx.doi.org/10.1016/j.ympev.2010.10.016.
Potts, A.L.J., Edderson, T.E.A.H., Rimm, G.U.W.G., 2014. Constructing phylogenies in the presence of intra-individual site polymorphisms (2ISPs) with a focus on the nuclear ribosomal cistron. Syst. Biol. 63, 1–16. http://dx.doi.org/10.5061/dryad.21jj2.
Rabosky, D.L., 2006. LASER: a maximum likelihood toolkit for detecting temporal shifts in diversification rates from molecular phylogenies. Evol. Bioinform. Online 2, 273–276. http://dx.doi.org/10.1554/05-424.1.
Rabosky, D.L., Lovette, I.J., 2008. Explosive evolutionary radiations: decreasing speciation or increasing extinction through time? Evolution (N. Y) 62, 1866–1875. http://dx.doi.org/10.1111/j.1558-5646.2008.00409.x.
Core Team, R., 2016. R: A language and environment for sta- tistical computing. R Foundation for Statistical Computing, Vienna, Austria Available at: https://www.R-project.org/.
Rambaut, A., Suchard, M., Xie, D., Drummond, A., 2014. Tracer v. 1.6. Institute of Evolutionary Biology, University of Edinburgh. Available online at: http://beast.bio.ed.ac.uk/Tracer.
Ree, R.H., Smith, S.A., 2008. Maximum likelihood inference of geographic range evolution by dispersal, local extinction, and cladogenesis. Syst. Biol. 57, 4–14.
Remsen, J.V., Areta, J.I., Cadena, C.D., Claramunt, S., Jaramillo, A., Pacheco, J.F., Pérez-Emán, J., Robbins, M.B., Stiles, F.G., Stotz, D.F., Zimmer., K.J., 2017. A classification of the bird species of South America. American Ornithologists' Union. [WWW Document]. Am. Ornithol. Union. URL http://www.museum.lsu.edu/~Remsen/SACCBaseline.htm.
Ribas, C.C., Miyaki, C.Y., 2007. Análise comparativa de padrões de diversificação em quatro gêneros de psitacídeos neotropicais. Rev. Bras. Ornitol. 15, 245–252.
Rice, N.H., 2005. Phylogenetic relationships of antpitta genera (Passeriformes: Formicariidae). Auk 122, 673. http://dx.doi.org/10.1642/0004-8038(2005)122[0673:PROAGP]2.0.CO;2.
Ridgway, R., 1909. New genera, species and subspecies of Formicariidae, Furnariidae, and Dendrocolaptidae. Proc. Biol. Soc. Washington 22, 69–74.
Ronquist, F., Sanmartín, I., 2011. Phylogenetic methods in biogeography. Annu. Rev. Ecol. Evol. Syst. 42, 441–464.
Ronquist, F., Teslenko, M., Van Der Mark, P., Ayres, D.L., Darling, A., Höhna, S., Larget, B., Liu, L., Suchard, M.A., Huelsenbeck, J.P., 2012. Mrbayes 3.2: efficient bayesian phylogenetic inference and model choice across a large model space. Syst. Biol. 61, 539–542. http://dx.doi.org/10.1093/sysbio/sys029.
Roy, S.M., 1997. Recent diversification in African greenbuls (Pycnonotidae: Andropadus) supports a montane speciation model. Proc. R. Soc. London B 264, 1337–1344.
Roy, S.M., da Silva, J.M.C., Arctander, P., Garcia-Moreno, J., Fjeldså, J., 1997. The role of montane regions in the speciation of South American and African birds. In: Mindell, D.P. (Ed.), Avian Mol. Evol. Syst. 325–343.
Rull, V., 2008. Speciation timing and neotropical biodiversity: The Tertiary-Quaternary debate in the light of molecular phylogenetic evidence. Mol. Ecol. 17, 2722–2729. http://dx.doi.org/10.1111/j.1365-294X.2008.03789.x.
Sanmartín, I., Van Der Mark, P., Ronquist, F., 2008. Inferring dispersal: a Bayesian approach to phylogeny-based island biogeography, with special reference to the Canary Islands. J. Biogeogr. 35, 428–449. http://dx.doi.org/10.1111/j.1365-2699.2008.01885.x.
Schweizer, M., Hertwig, S.T., Seehausen, O., 2014. Diversity versus disparity and the role of ecological opportunity in a continental bird radiation. J. Biogeogr. 41, 1301–1312. http://dx.doi.org/10.1111/jbi.12293.
Scotti-saintagne, C., Dick, C.W., Caron, H., Sire, P., Vendramin, G.G., Casalis, M., Buonamici, A., Valencia, R., Lemes, M.R., Gribel, R., Scotti, I., Biogeco, I.U.M.R., Cedex, C., Genetica, I., Firenze, S., Ricerche, N., 2013. Amazon diversification and cross- Andean dispersal of the widespread Neotropical tree species Jacaranda copaia (Bignoniaceae). J. Biogeogr. 40, 707–719. http://dx.doi.org/10.1111/j.1365-2699.2012.02797.x.
Sedano, R.E., Burns, K.J., 2010. Are the Northern Andes a species pump for Neotropical birds? Phylogenetics and biogeography of a clade of Neotropical tanagers (Aves: Thraupini). J. Biogeogr. 37, 325–343. http://dx.doi.org/10.1111/j.1365-2699.2009.02200.x.
Smith, B.T., Klicka, J., 2010. The profound influence of the Late Pliocene Panamanian uplift on the exchange, diversification, and distribution of New World birds. Ecography (Cop.) 33, 333–342. http://dx.doi.org/10.1111/j.1600-0587.2009.06335.x.
Smith, B.T., McCormack, J.E., Cuervo, A.M., Hickerson, M.J., Aleixo, A., Burney, C.W., Xie, X., Harvey, M.G., Faircloth, B.C., Cadena, C.D., Pérez-Emán, J., Glenn, T.C., Derryberry, E.P., Prejean, J., Fields, S., Brumfield, R.T., 2014. The drivers of tropical speciation. Nature. http://dx.doi.org/10.1038/nature13687.
Sorenson, M.D., Ast, J.C., Dimcheff, D.E., Yuri, T., Mindell, D.P., 1999. Primers for a PCR-based approach to mitochondrial genome sequencing in birds and other vertebrates. Mol. Phylogenet. Evol. 12, 105–114. http://dx.doi.org/10.1006/mpev.1998.0602.
Stratford, J.a., Stouffer, P.C., 2015. Forest fragmentation alters microhabitat availability for Neotropical terrestrial insectivorous birds. Biol. Conserv. 1–7. http://dx.doi.org/10.1016/j.biocon.2015.01.017.
Teixeira, M., Prates, I., Nisa, C., Silva-Martins, N.S.C., Strüssmann, C., Rodrigues, M.T., 2016. Molecular data reveal spatial and temporal patterns of diversification and a cryptic new species of lowland Stenocercus Duméril and Bibron, 1837 (Squamata: Tropiduridae). Mol. Phylogenet. Evol. 94, 410–423. http://dx.doi.org/10.1016/j.ympev.2015.09.010.
Tobias, J.a., Bates, J.M., Hackett, S.J., Seddon, N., 2008. Comment on "The latitudinal gradient in recent speciation and extinction rates of birds and mammals". Science 319, 901. http://dx.doi.org/10.1126/science.1150828.
Wagenmakers, E.-J., Farrell, S., 2004. AIC model selection using Akaike weights. Psychon. Bull. Rev. 11, 192–196. http://dx.doi.org/10.3758/BF03206482.
Weir, J.T., 2006. Divergent timing and patterns of species accumulation in lowland and highland neotropical birds. Evolution (N. Y). 60, 842–855. http://dx.doi.org/10.1111/j.0014-3820.2006.tb01161.x.
Weir, J.T., Price, M., 2011. Andean uplift promotes lowland speciation through vicariance and dispersal in Dendrocincla woodcreepers. Mol. Ecol. 20, 4550–4563. http://dx.doi.org/10.1111/j.1365-294X.2011.05294.x.
Weir, J.T., Schluter, D., 2004. Ice sheets promote specia- tion in boreal birds. Proc. R. Soc. B Biol. Sci. 271, 1881–1887.
Wesselingh, F.P., Räsänen, M.E., Irion, G., Vonhof, H.B., Kaandorp, R., Renema, W., Romero Pittman, L., Gingras, M., 2002. Lake Pebas: a palaeoecological reconstruction of a Miocene, long-lived lake complex in western Amazonia. Cainozoic Res. 1, 35–81.
Whitney, B.M., Pacheco, J.F., Isler, P.R., Isler, M.L., 1995. Hylopezus nattereri (Pinto, 1937) is a valid species (Passeriformes, Formicariidae). Ararajuba.
Wiens, J.J., Moen, D.S., 2008. Missing data and the accuracy of Bayesian phylogenetics 46, 307–314. doi: 10.3724/SP.J.1002.2008.08040.
Winger, B.M., Hosner, P.A., Bravo, G.A., Cuervo, A.M., Aristizábal, N., Cueto, L.E., Bates, J.M., 2015. Inferring speciation history in the Andes with reduced-representation sequence data: an example in the bay-backed antpittas (Aves; Grallariidae; Grallaria hypoleuca s. l.). Mol. Ecol. 24, 6256–6277. http://dx.doi.org/10.1111/mec.13477.
Zachos, J., Pagani, M., Sloan, L., Thomas, E., Billups, K., 2001. Trends, rhythms, and aberrations in global climate 65 Ma to present. Science 292, 686–693. http://dx.doi.org/10.1126/science.1059412.